

# **Tomographic models based on pixels and matrices**

**Samuli Siltanen**

PhD Winter School 2023

Advanced methods for mathematical image analysis

Bologna, Italy

January 24, 2023

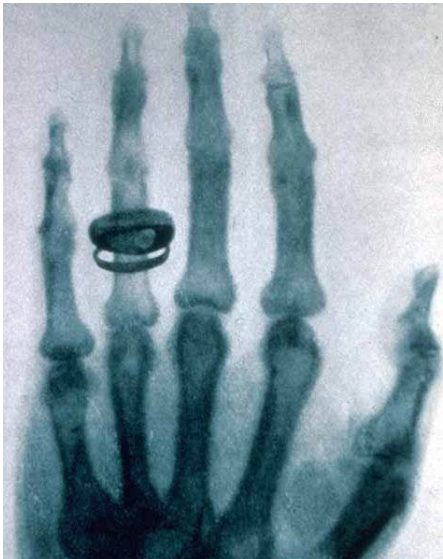


Instagram:  
@samuntiede  
@monday\_spider

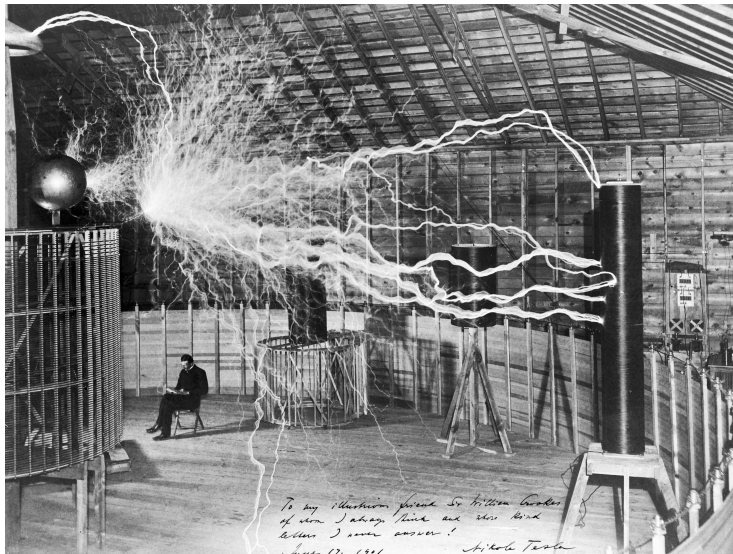


YouTube:  
@professor\_sam  
@Samuntiedekanava

**Wilhelm Conrad Röntgen invented X-rays and was awarded the first Nobel Prize in Physics in 1901**



# But even before Röntgen, Nikola Tesla had observed X-rays in his own way



# Outline

## Why pixel-based tomographic modelling?

Restricted time → sparse tomography

Restricted radiation dose → sparse tomography

Restricted money → sparse tomography

## The Beer-Lambert Law

## Pixel-based measurement model

Matrix model for sparse tomography

Transpose of  $A$ : backprojection

Ill-posedness of sparse tomography

Total variation regularization

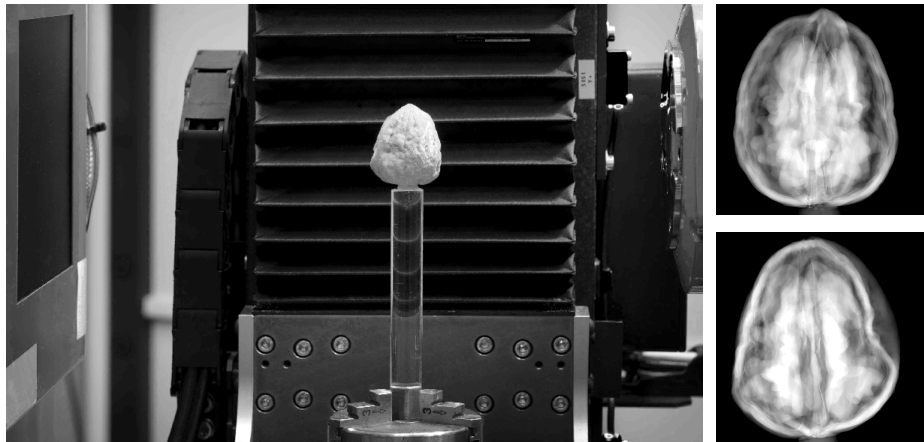
## Regularization

Tikhonov regularization

Total variation regularization

Frame-sparsity methods

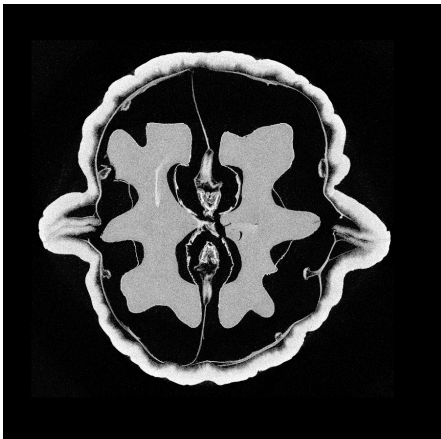
# We collected X-ray projection data of a walnut from 1200 directions



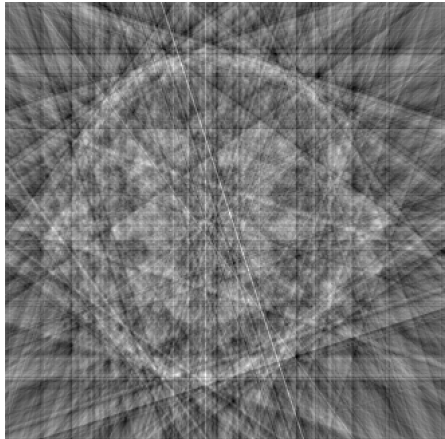
Data collection: thanks to Keijo Hämäläinen and Aki Kallonen, University of Helsinki.

The data is openly available at <http://fips.fi/dataset.php>, thanks to Esa Niemi and Antti Kujanpää

# Reconstructions of a 2D slice through the walnut using filtered back-projection (FBP)

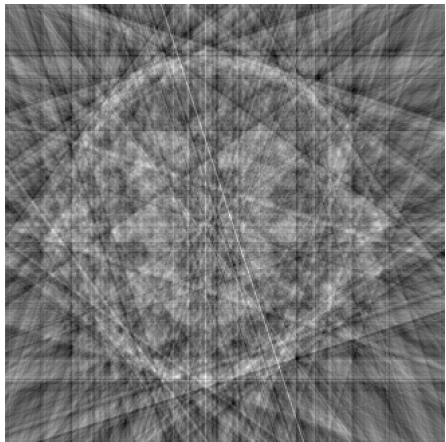


FBP with comprehensive data  
(1200 projections)

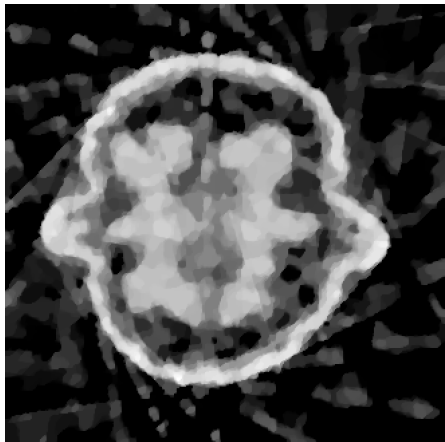


FBP with sparse data  
(20 projections)

# Sparse-data reconstruction of the walnut using non-negative total variation regularization



Filtered back-projection

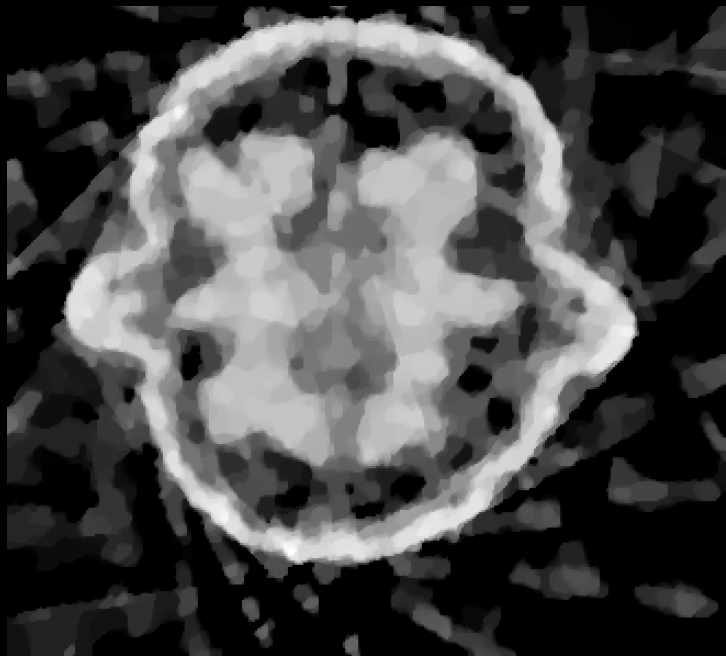


Constrained TV regularization  
$$\arg \min_{f \in \mathbb{R}_+^n} \{ \|Af - m\|_2^2 + \alpha \|\nabla f\|_1 \}$$

# Haar wavelet sparsity reconstruction



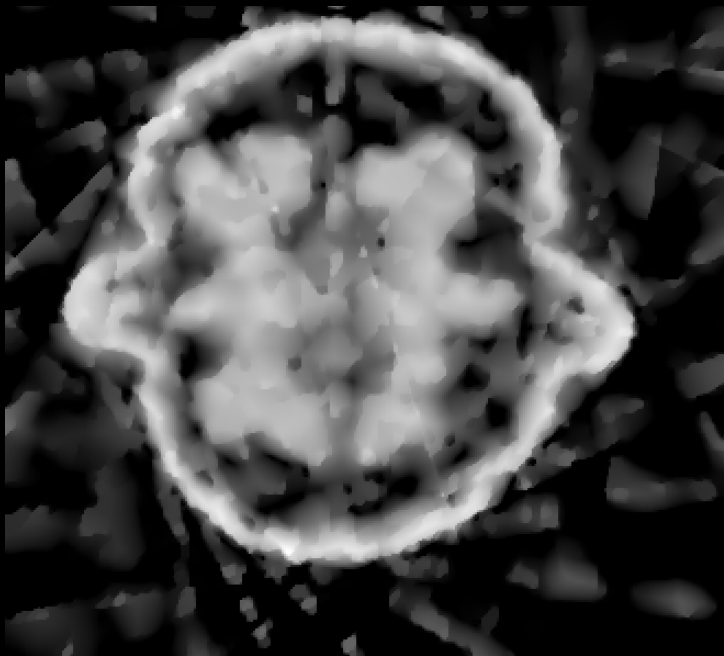
# Total Variation (TV) reconstruction



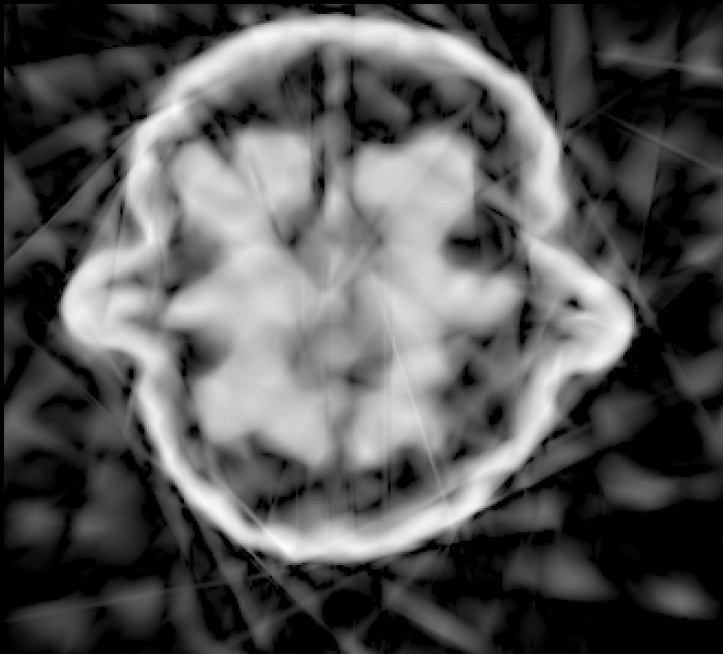
## Daubechies 2 wavelet sparsity reconstruction

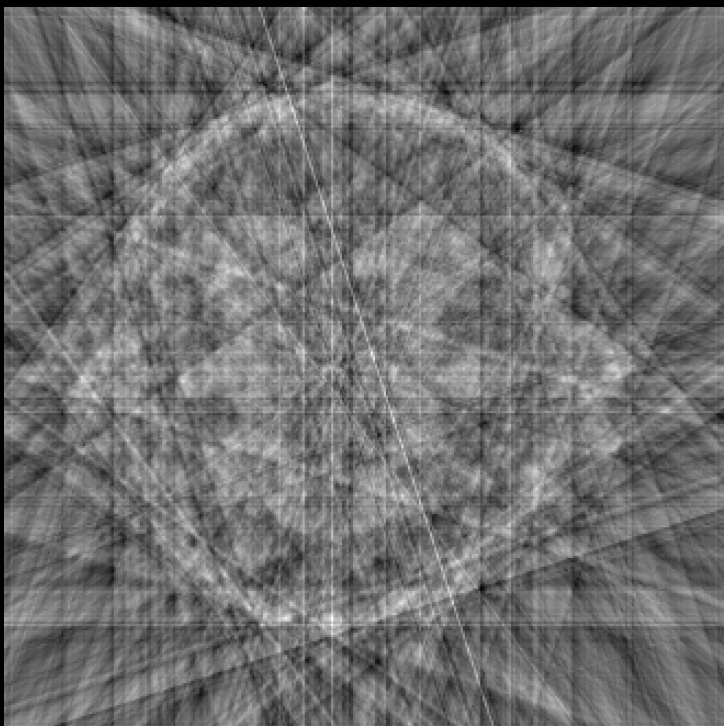


# Total Generalized Variation (TGV) reconstruction



# Shearlet sparsity reconstruction





# Outline

## Why pixel-based tomographic modelling?

Restricted time → sparse tomography

Restricted radiation dose → sparse tomography

Restricted money → sparse tomography

## The Beer-Lambert Law

## Pixel-based measurement model

Matrix model for sparse tomography

Transpose of  $A$ : backprojection

Ill-posedness of sparse tomography

Total variation regularization

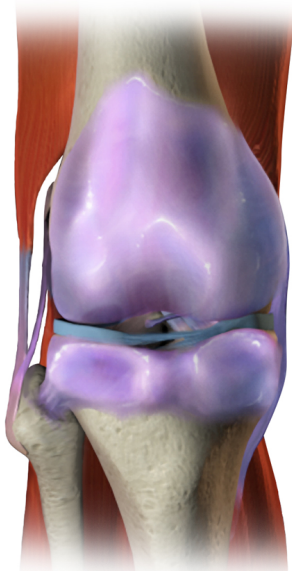
## Regularization

Tikhonov regularization

Total variation regularization

Frame-sparsity methods

Normal Knee



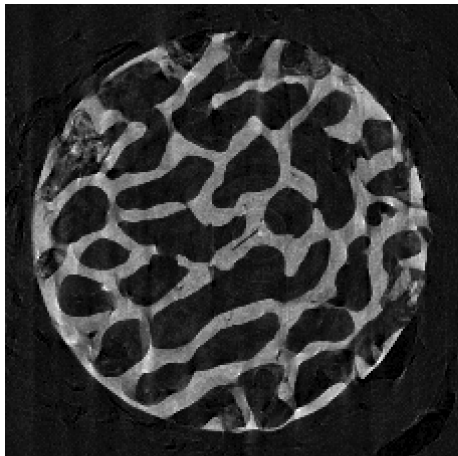
Osteoarthritis



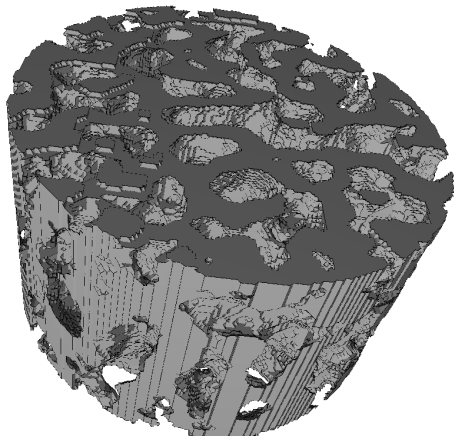
Image by Bruce Blaus, CC BY-SA 4.0

<https://commons.wikimedia.org/w/index.php?curid=44968165>

We consider small specimens of human bone imaged using microtomography

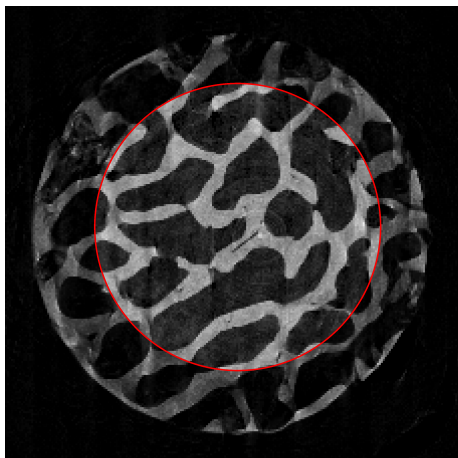


Slice of 3D reconstruction by FDK based on **596 angles**



Three-dimensional structure

We pick out a smaller region of interest  
for osteoarthritis analysis



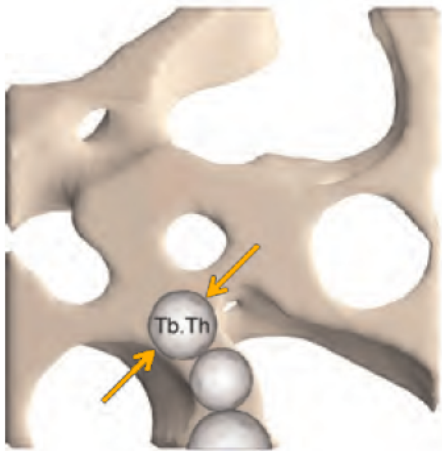
Slice of 3D reconstruction by FDK  
based on **596 angles**



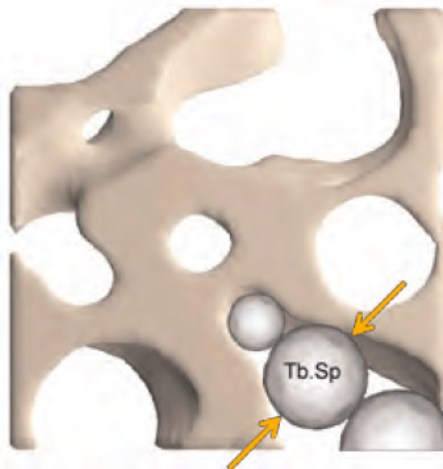
Slice of 3D region of interest  
after binary thresholding

We use two numerical quality measures applied to segmented three-dimensional bone structure

Trabecular thickness



Trabecular separation



[Bouxsein, Boyd, Christiansen, Guldberg, Jepsen, & Müller 2010]

The goal is to reduce measurement time  
by recording fewer radiographs



3D FDK reconstruction  
based on **40 angles**



3D shearlet-sparsity reconstruction  
based on **40 angles**

# Bone quality parameters from ground truth



Projections: 300

**Thickness**

0.34

**Separation**

0.71



Projections: 300

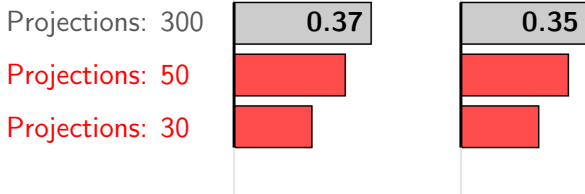
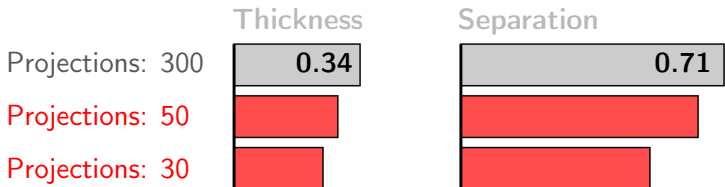
**Thickness**

0.37

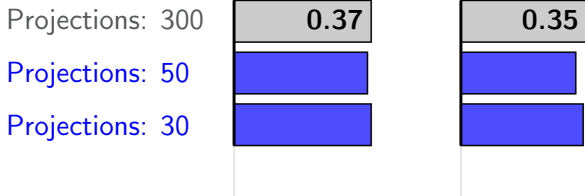
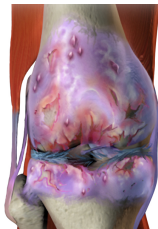
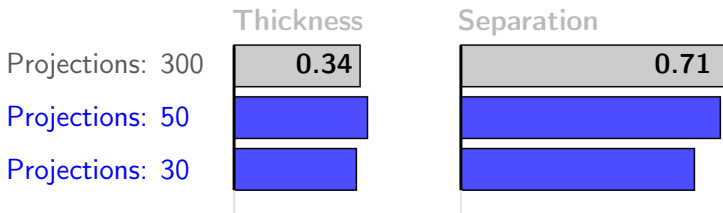
**Separation**

0.35

# Results from FDK reconstructions



# Results from 3D shearlet-sparsity reconstructions



# The osteoarthritis project was a joint work with

**Tatiana Bubba**, University of Helsinki, Finland

**Sakari Karhula**, Oulu University Hospital, Finland

**Juuso Ketola**, Oulu University Hospital, Finland

**Maximilian März**, TU Berlin

**Miika T. Nieminen**, University of Oulu, Finland

**Zenith Purisha**, University of Helsinki, Finland

**Juho Rimpeläinen**, University of Helsinki, Finland

**Simo Saarakkala**, Oulu University Hospital, Finland

# Outline

## Why pixel-based tomographic modelling?

Restricted time → sparse tomography

**Restricted radiation dose → sparse tomography**

Restricted money → sparse tomography

## The Beer-Lambert Law

## Pixel-based measurement model

Matrix model for sparse tomography

Transpose of  $A$ : backprojection

Ill-posedness of sparse tomography

Total variation regularization

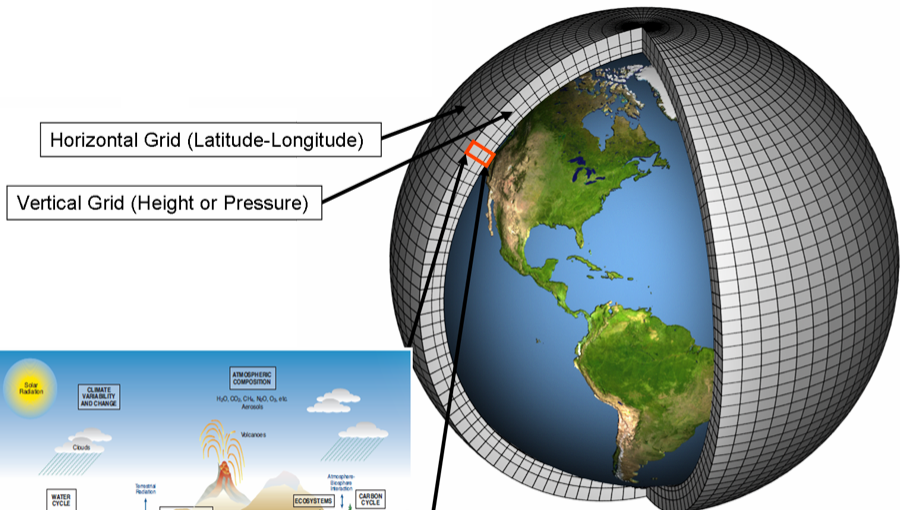
## Regularization

Tikhonov regularization

Total variation regularization

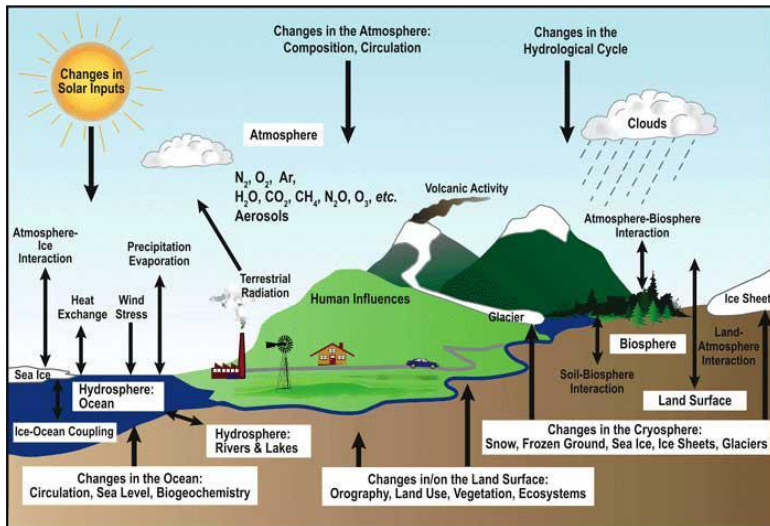
Frame-sparsity methods

# Climate change is predicted using climate models



Source: Wikipedia

# Climata models have a lot of details, and plant metabolism is crucial to model accurately

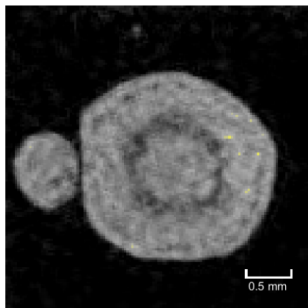


**Tomography study jointly with physicists,  
biologists, radiochemists and climate scientists**

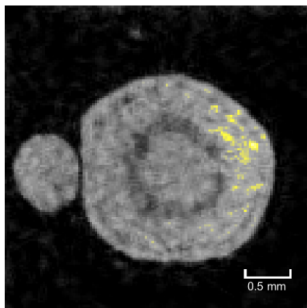


# Time-dependent sparse tomography reveals the movement of iodine in the phloem

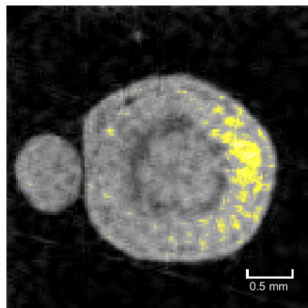
0 minutes



166 minutes



235 minutes



# Outline

## Why pixel-based tomographic modelling?

Restricted time → sparse tomography

Restricted radiation dose → sparse tomography

Restricted money → sparse tomography

## The Beer-Lambert Law

## Pixel-based measurement model

Matrix model for sparse tomography

Transpose of  $A$ : backprojection

Ill-posedness of sparse tomography

Total variation regularization

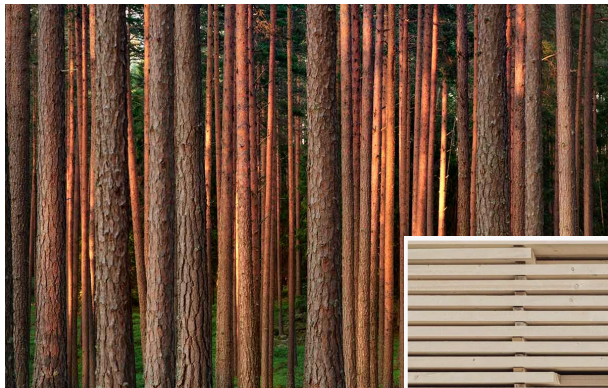
## Regularization

Tikhonov regularization

Total variation regularization

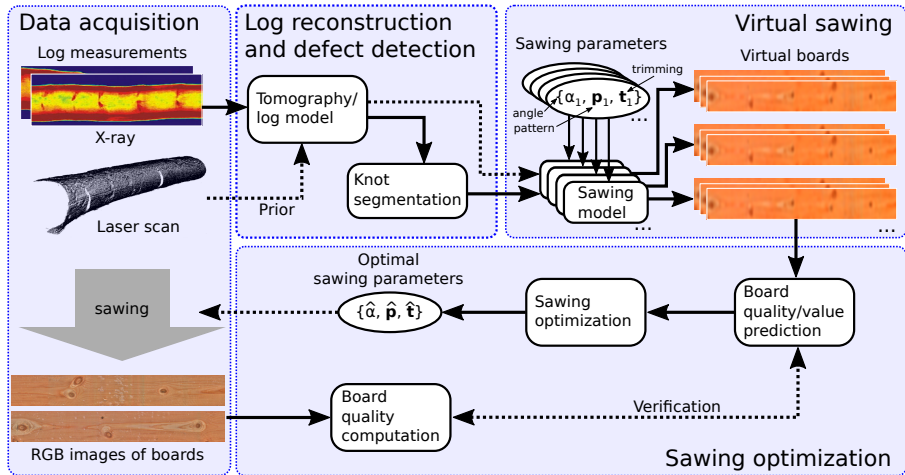
Frame-sparsity methods

The next example of sparse-data tomography  
is about sawing tree trunks into planks



Pictures: Stora Enso

# The sawmill industry wants to cut tree trunks so that the amount of material produced is maximal



Picture courtesy of Sebastian Springer and Andreas Hauptmann

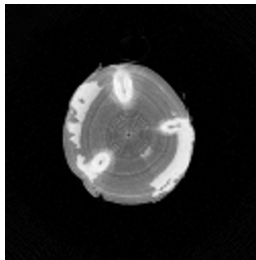
# Finnish spin-off company Finnos designs X-ray imaging devices for sawing



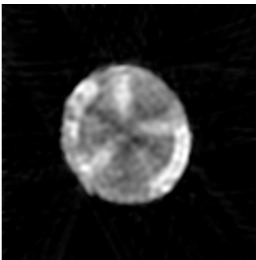
Picture: Finnos

# Each angle needs X-ray source → sparse data

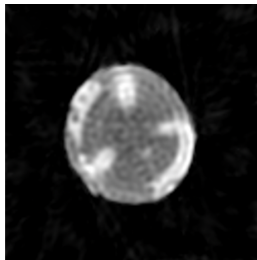
Reference  
360 angles



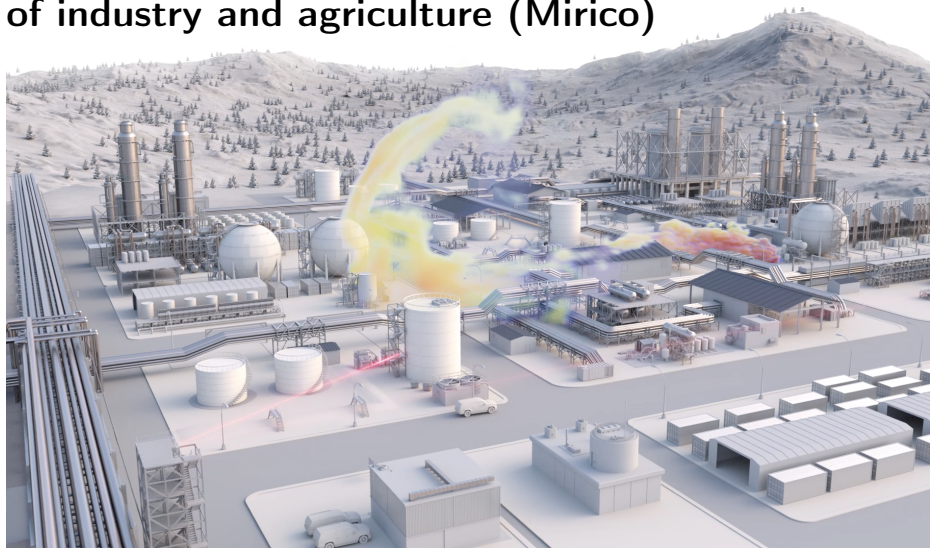
Kalman filter  
3 angles



Kalman filter  
9 angles



# Laser tomography enables monitoring gases of industry and agriculture (Mirico)



# Laser tomography enables monitoring gases of industry and agriculture (Mirico)



# Outline

## Why pixel-based tomographic modelling?

Restricted time → sparse tomography

Restricted radiation dose → sparse tomography

Restricted money → sparse tomography

## The Beer-Lambert Law

### Pixel-based measurement model

Matrix model for sparse tomography

Transpose of  $A$ : backprojection

Ill-posedness of sparse tomography

Total variation regularization

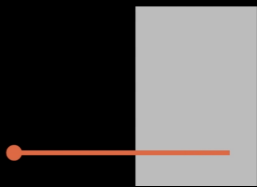
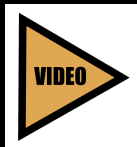
### Regularization

Tikhonov regularization

Total variation regularization

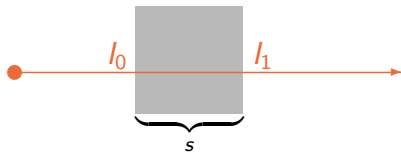
Frame-sparsity methods

X-ray intensity attenuates inside matter,  
here shown with a homogeneous block



# Formula for X-ray attenuation along a line inside homogeneous matter

An X-ray with intensity  $I_0$  enters a homogeneous physical body.

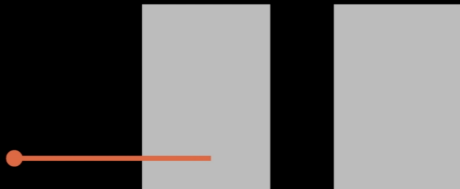
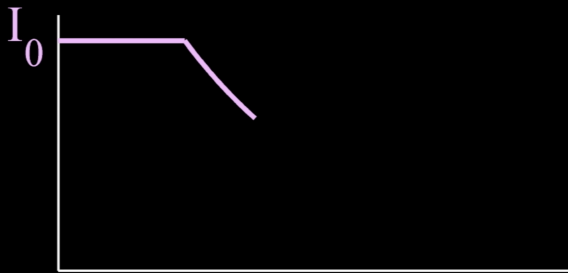
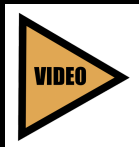


The intensity  $I_1$  of the X-ray when it exits the material is

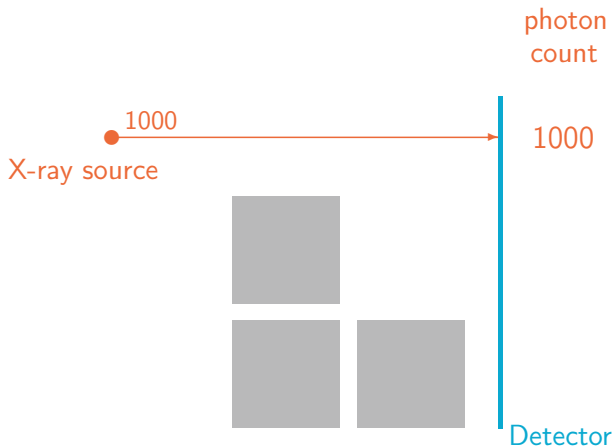
$$I_1 = I_0 e^{-\mu s},$$

where  $s$  is the length of the path of the X-ray inside the body and  $\mu > 0$  is X-ray attenuation coefficient.

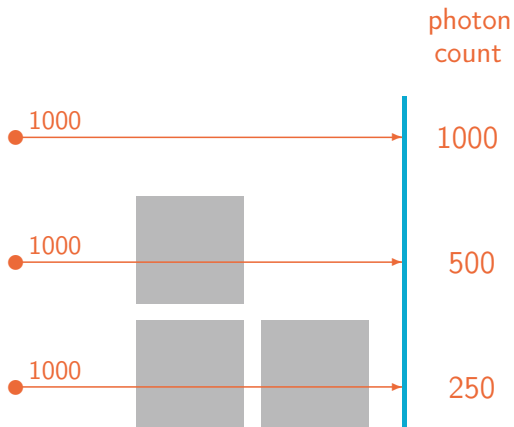
X-ray intensity attenuates inside matter,  
here shown with two homogeneous blocks



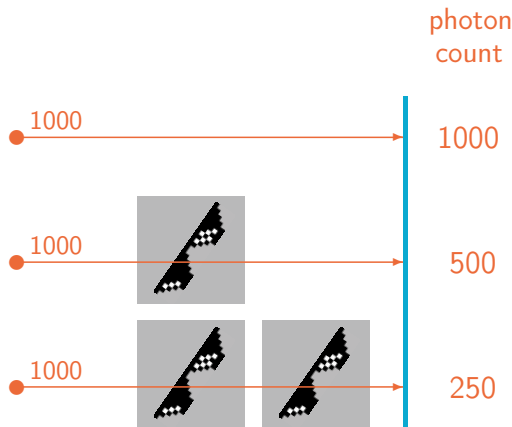
A digital X-ray detector counts how many photons arrive at each pixel



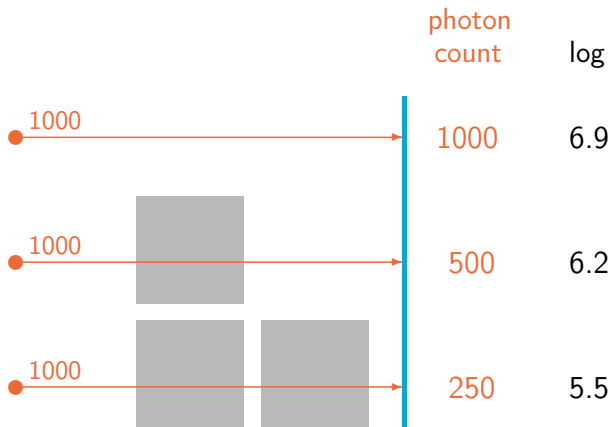
# Adding material between the source and detector reveals the exponential X-ray attenuation law



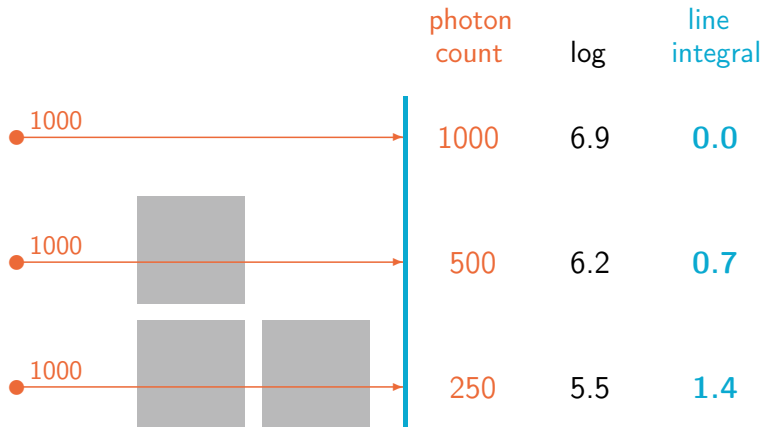
# Physical material kind of acts as “sunglasses” for X-rays



We take logarithm of the photon counts to compensate for the exponential attenuation law



Final calibration step is to subtract the logarithms from the empty space value (here 6.9)



# Formula for X-ray attenuation along a line: Beer-Lambert law

Let  $f : [a, b] \rightarrow \mathbb{R}$  be a nonnegative function modelling X-ray attenuation along a line inside a physical body.

Beer-Lambert law connects the initial and final intensities:

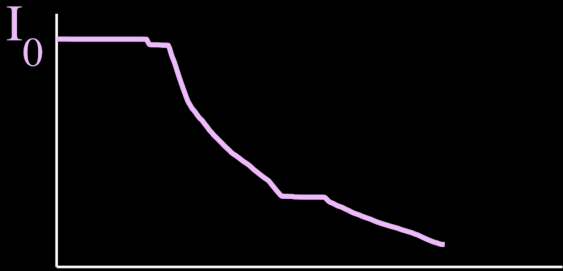
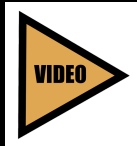
$$I_1 = I_0 e^{-\int_a^b f(x)dx}.$$

We can also write it in the form

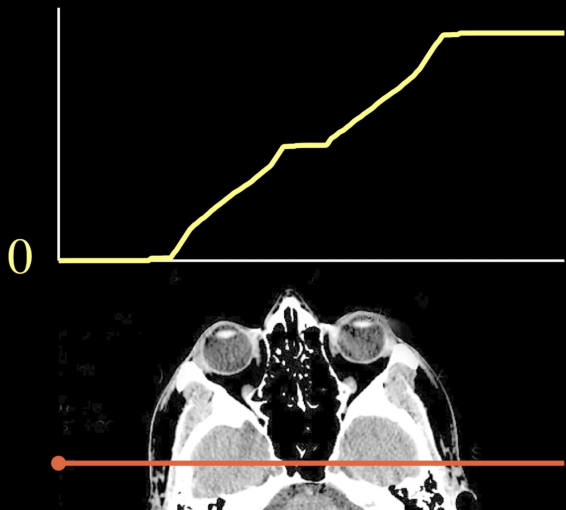
$$-\log(I_1/I_0) = \int_a^b f(x)dx,$$

where  $I_0$  is known from calibration and  $I_1$  from measurement.

Attenuation process is complicated inside a head because there are different tissues



After calibration we are observing how much attenuating matter the X-ray encounters in



# Outline

## Why pixel-based tomographic modelling?

Restricted time → sparse tomography

Restricted radiation dose → sparse tomography

Restricted money → sparse tomography

## The Beer-Lambert Law

## Pixel-based measurement model

Matrix model for sparse tomography

Transpose of  $A$ : backprojection

Ill-posedness of sparse tomography

Total variation regularization

## Regularization

Tikhonov regularization

Total variation regularization

Frame-sparsity methods

# Outline

## Why pixel-based tomographic modelling?

Restricted time → sparse tomography

Restricted radiation dose → sparse tomography

Restricted money → sparse tomography

## The Beer-Lambert Law

## Pixel-based measurement model

Matrix model for sparse tomography

Transpose of  $A$ : backprojection

Ill-posedness of sparse tomography

Total variation regularization

## Regularization

Tikhonov regularization

Total variation regularization

Frame-sparsity methods

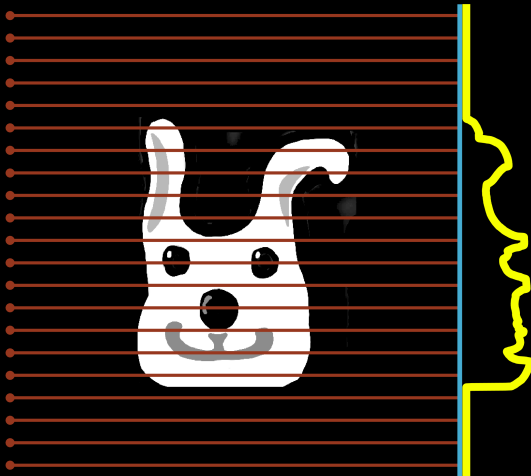
Our test example is a cartoon bunny image.  
We simulate projection data along 11 directions



1024×1024 pixels

0.0°

Angle 1



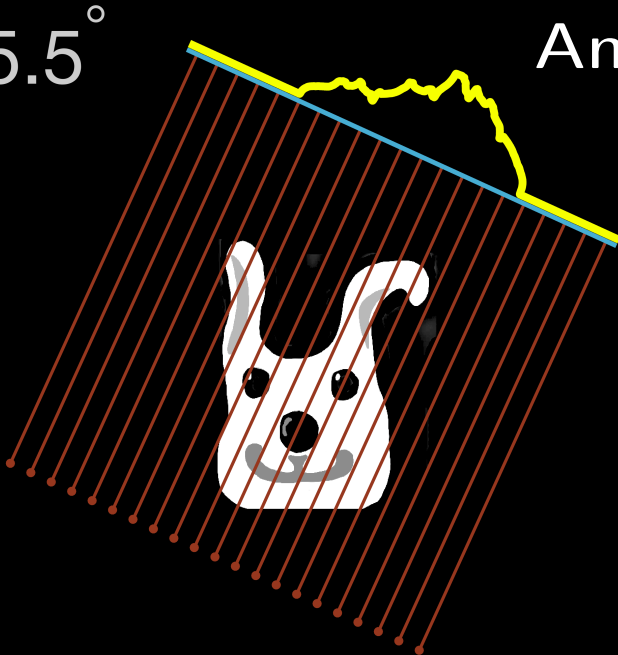
$32.7^\circ$

Angle 2



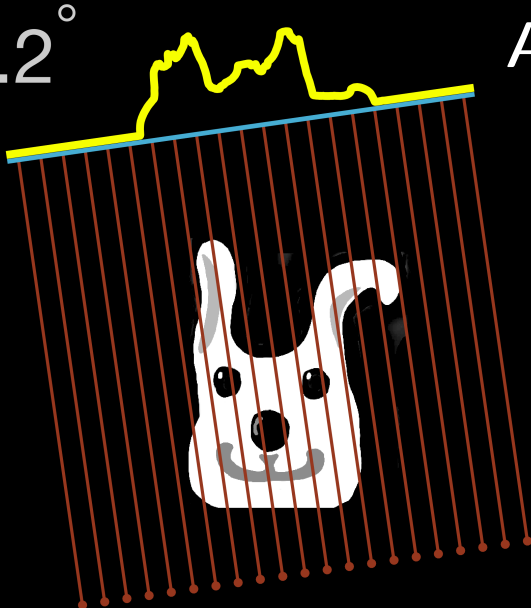
$65.5^{\circ}$

Angle 3



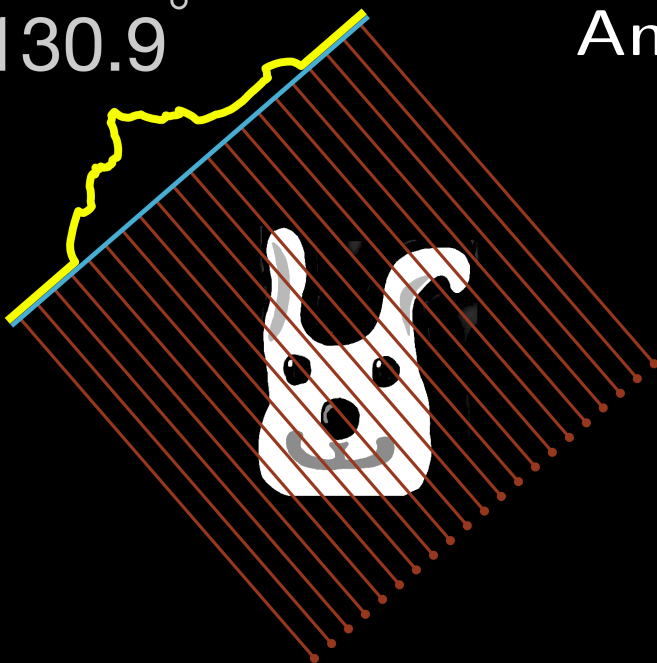
98.2°

Angle 4



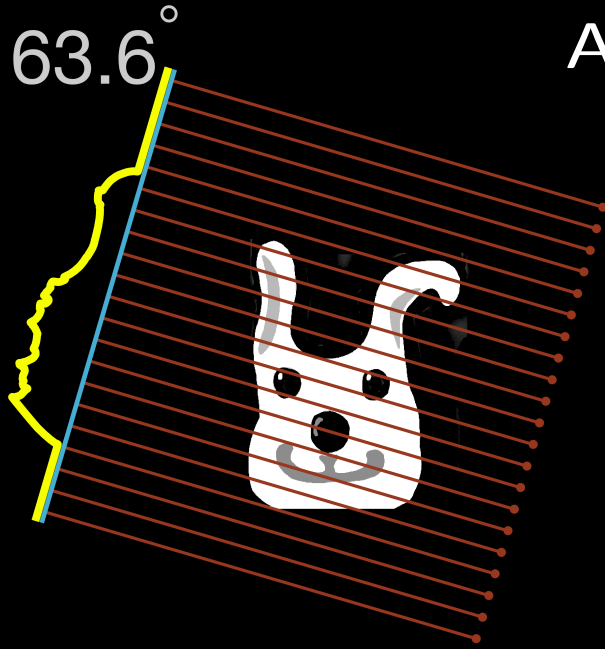
130.9°

Angle 5



163.6°

Angle 6



196.4°

Angle 7



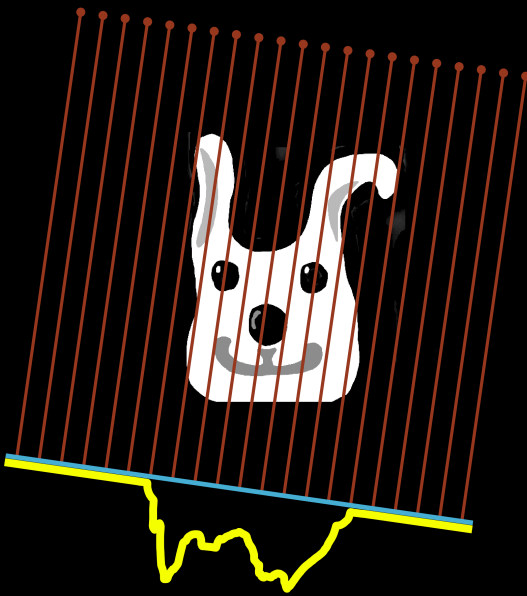
$229.1^\circ$

Angle 8



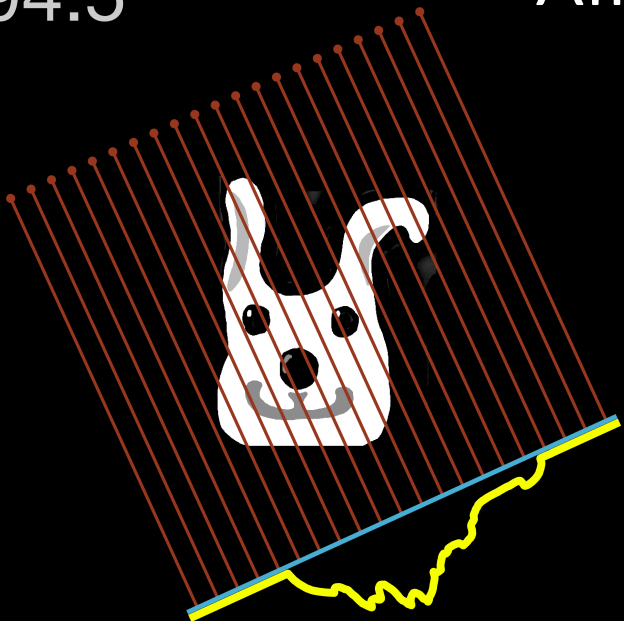
261.8°

Angle 9



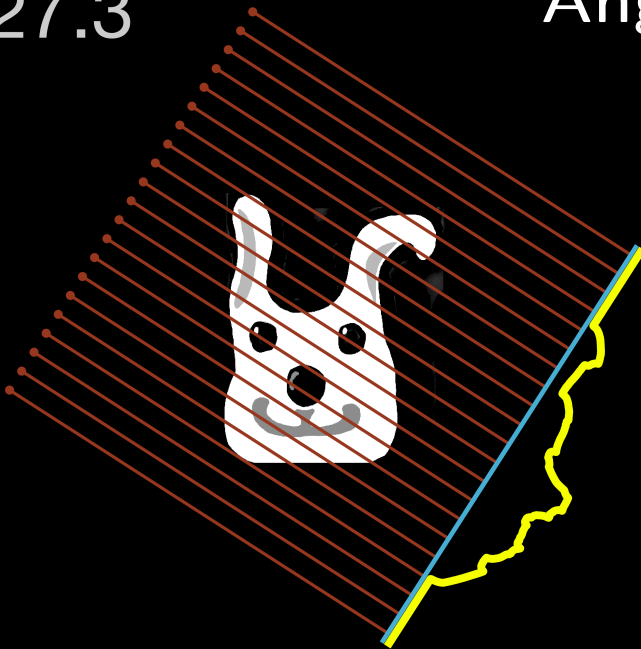
294.5°

Angle 10



$327.3^{\circ}$

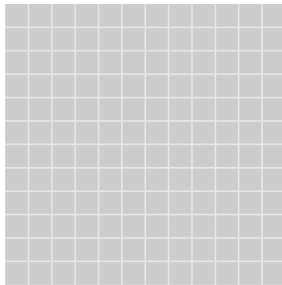
Angle 11



Discretize the unknown by dividing it into pixels;  
this is necessary for finite computation



Target (unknown)



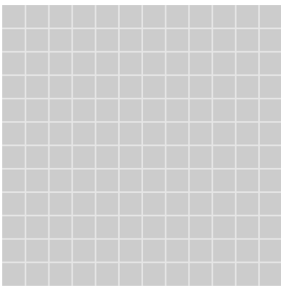
12×12 pixel grid

$x_1$	$x_{13}$	$x_{25}$	$x_{37}$	$x_{49}$	$x_{61}$	$x_{73}$	$x_{85}$	$x_{97}$	$x_{109}$	$x_{121}$	$x_{133}$
$x_2$	$x_{14}$	$x_{26}$	$x_{38}$	$x_{50}$	$x_{62}$	$x_{74}$	$x_{86}$	$x_{98}$	$x_{110}$	$x_{122}$	$x_{134}$
$x_3$	$x_{15}$	$x_{27}$	$x_{39}$	$x_{51}$	$x_{63}$	$x_{75}$	$x_{87}$	$x_{99}$	$x_{111}$	$x_{123}$	$x_{135}$
$x_4$	$x_{16}$	$x_{28}$	$x_{40}$	$x_{52}$	$x_{64}$	$x_{76}$	$x_{88}$	$x_{100}$	$x_{112}$	$x_{124}$	$x_{136}$
$x_5$	$x_{17}$	$x_{29}$	$x_{41}$	$x_{53}$	$x_{65}$	$x_{77}$	$x_{89}$	$x_{101}$	$x_{113}$	$x_{125}$	$x_{137}$
$x_6$	$x_{18}$	$x_{30}$	$x_{42}$	$x_{54}$	$x_{66}$	$x_{78}$	$x_{90}$	$x_{102}$	$x_{114}$	$x_{126}$	$x_{138}$
$x_7$	$x_{19}$	$x_{31}$	$x_{43}$	$x_{55}$	$x_{67}$	$x_{79}$	$x_{91}$	$x_{103}$	$x_{115}$	$x_{127}$	$x_{139}$
$x_8$	$x_{20}$	$x_{32}$	$x_{44}$	$x_{56}$	$x_{68}$	$x_{80}$	$x_{92}$	$x_{104}$	$x_{116}$	$x_{128}$	$x_{140}$
$x_9$	$x_{21}$	$x_{33}$	$x_{45}$	$x_{57}$	$x_{69}$	$x_{81}$	$x_{93}$	$x_{105}$	$x_{117}$	$x_{129}$	$x_{141}$
$x_{10}$	$x_{22}$	$x_{34}$	$x_{46}$	$x_{58}$	$x_{70}$	$x_{82}$	$x_{94}$	$x_{106}$	$x_{118}$	$x_{130}$	$x_{142}$
$x_{11}$	$x_{23}$	$x_{35}$	$x_{47}$	$x_{59}$	$x_{71}$	$x_{83}$	$x_{95}$	$x_{107}$	$x_{119}$	$x_{131}$	$x_{143}$
$x_{12}$	$x_{24}$	$x_{36}$	$x_{48}$	$x_{60}$	$x_{72}$	$x_{84}$	$x_{96}$	$x_{108}$	$x_{120}$	$x_{132}$	$x_{144}$

Then we aim for best possible reconstruction at the resolution provided by the grid



Target (unknown)



12×12 pixel grid



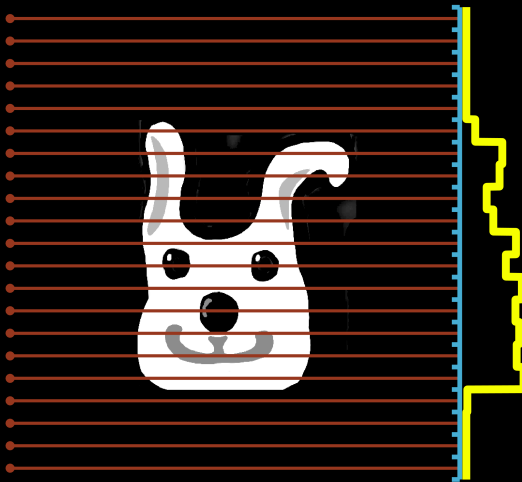
Desired reconstruction  
(downsampled target)

## We need to model the finite detector

Our simulated detector has 21 pixels. This number comes from the structure of the Matlab routine `radon.m` applied to a phantom of size  $12 \times 12$ .

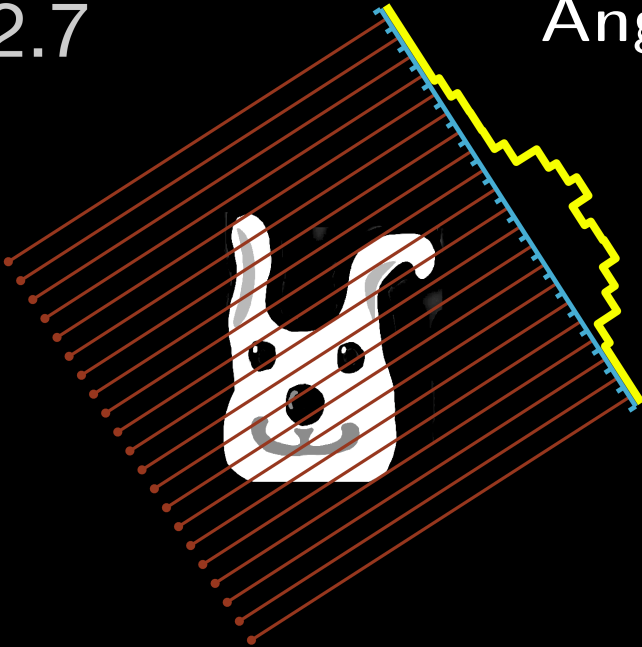
0.0°

Angle 1



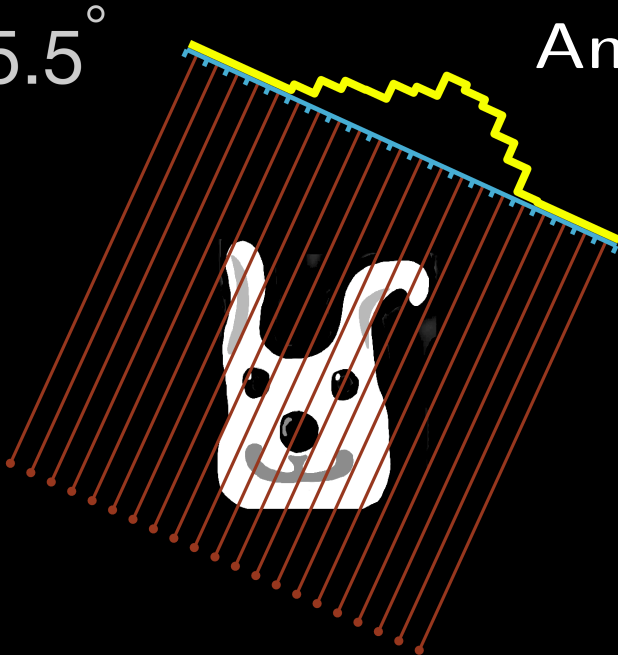
$32.7^\circ$

Angle 2



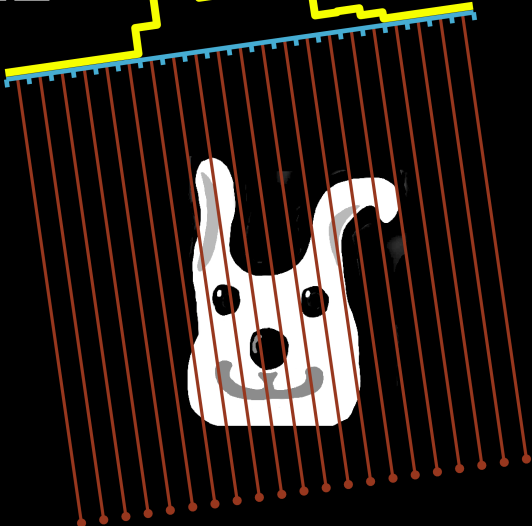
65.5°

Angle 3



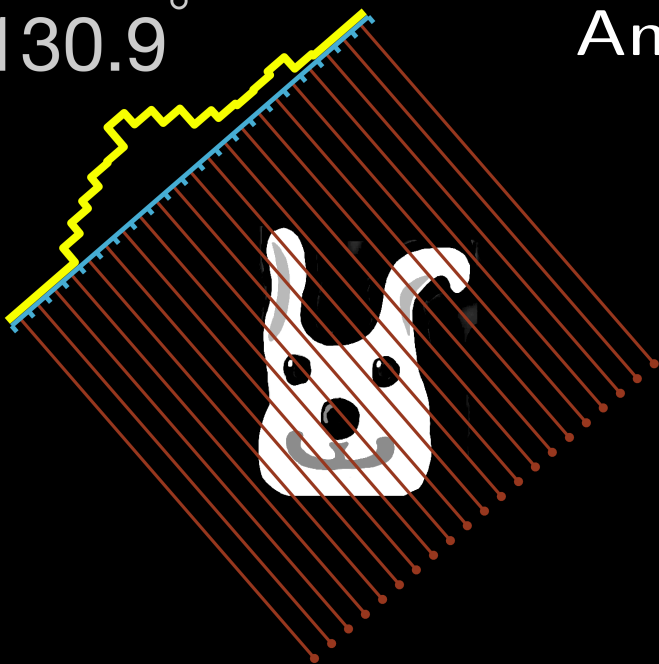
98.2°

Angle 4



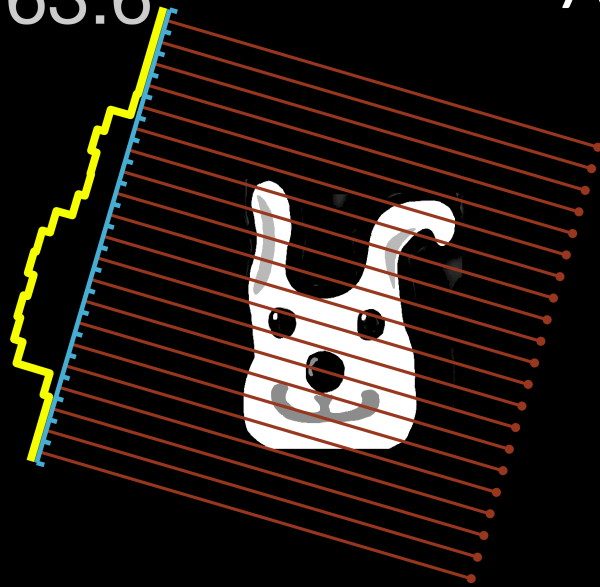
130.9°

Angle 5



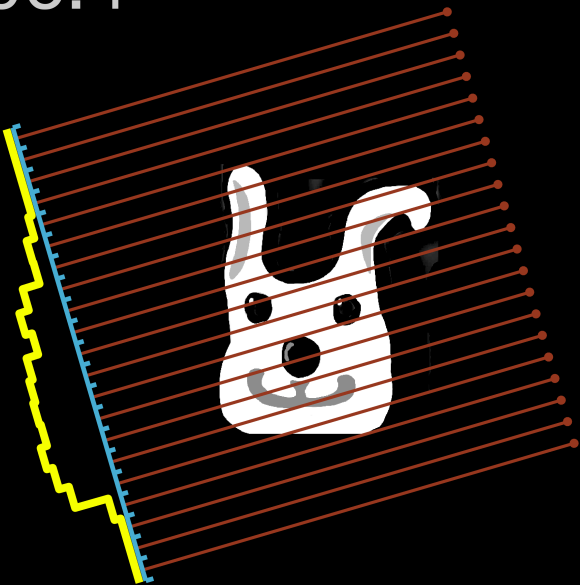
163.6°

Angle 6



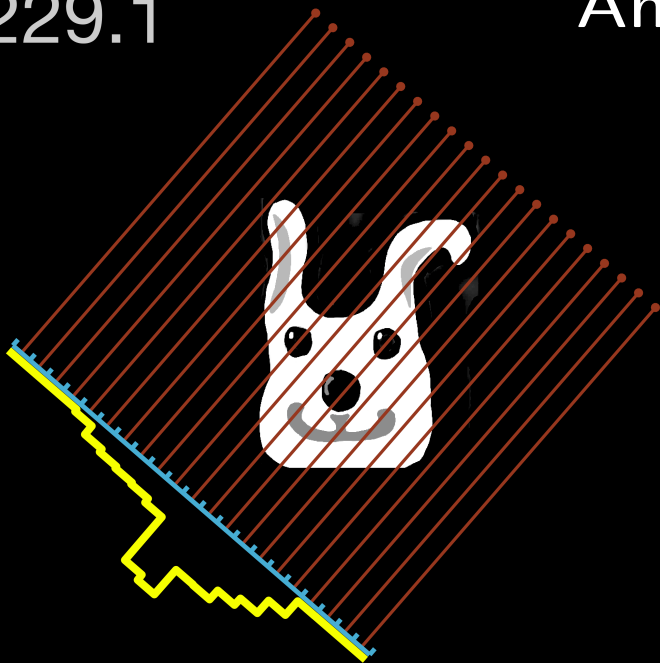
196.4°

Angle 7



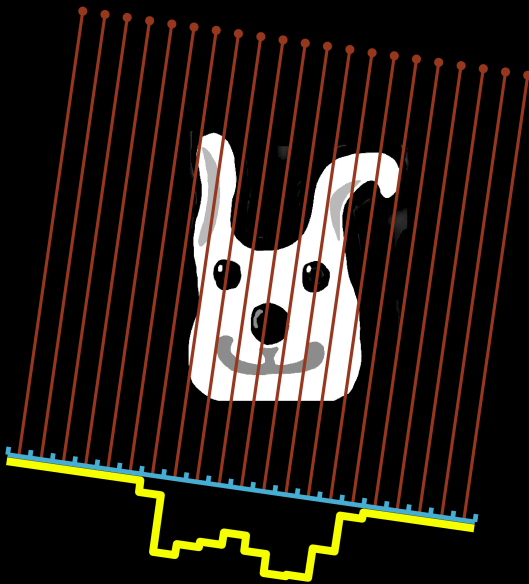
$229.1^\circ$

Angle 8



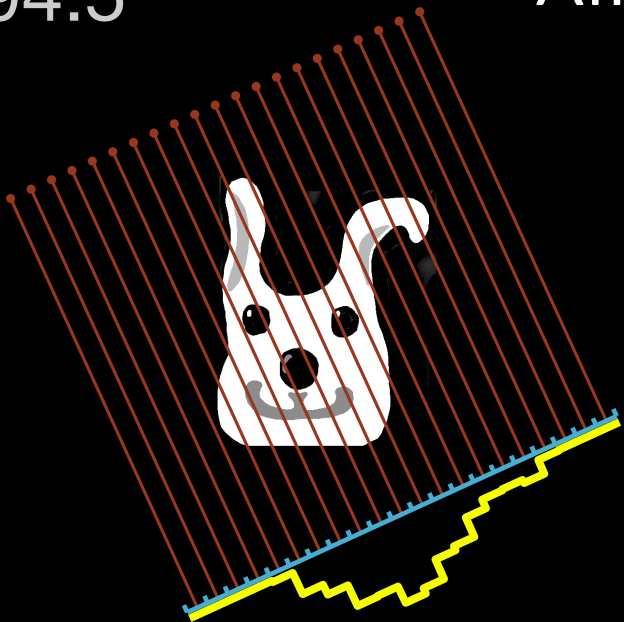
261.8°

Angle 9



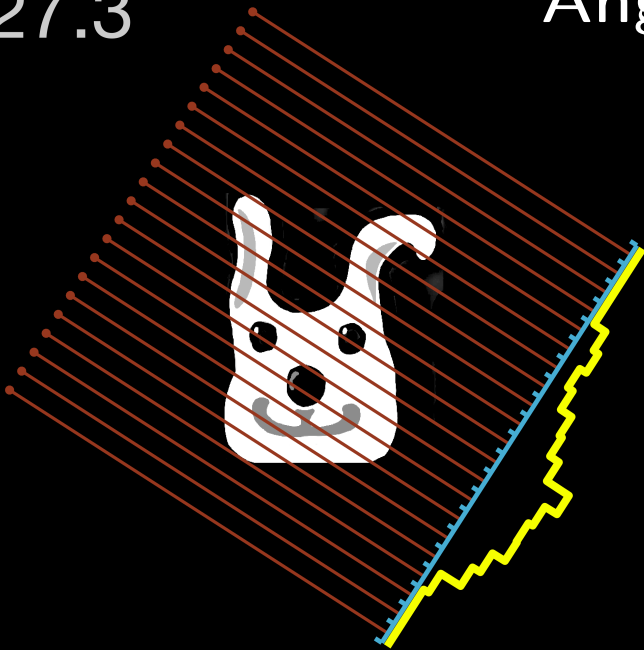
$294.5^\circ$

Angle 10



327.3°

Angle 11



## Let us build a discrete model for the 11-angle measurement shown above

We have 11 directions and 21 X-rays for each direction.

Every X-ray corresponds to one row in the matrix.

Therefore, our system matrix  $A$  has  $11 \cdot 21 = \text{231 rows}$ .

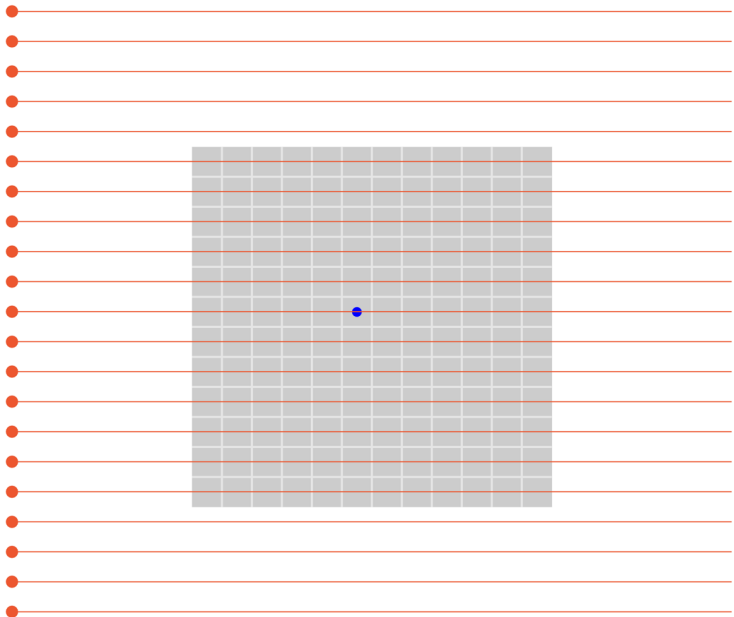
Our unknown image has  $12 \times 12 = 144$  pixels, and consequently the matrix  $A$  has **144 columns**.

Denote  $x \in \mathbb{R}^{144}$  and  $m \in \mathbb{R}^{231}$ . The matrix model is

$$Ax = m.$$

Next we see how to construct the matrix  $A$ .

# Measurement direction 1



# Paths of X-rays numbered from 1 to 9

1

2

3

4

5

6

$x_1$	$x_{13}$	$x_{25}$	$x_{37}$	$x_{49}$	$x_{61}$	$x_{73}$	$x_{85}$	$x_{97}$	$x_{109}$	$x_{121}$	$x_{133}$
-------	----------	----------	----------	----------	----------	----------	----------	----------	-----------	-----------	-----------

7

$x_2$	$x_{14}$	$x_{26}$	$x_{38}$	$x_{50}$	$x_{62}$	$x_{74}$	$x_{86}$	$x_{98}$	$x_{110}$	$x_{122}$	$x_{134}$
-------	----------	----------	----------	----------	----------	----------	----------	----------	-----------	-----------	-----------

8

$x_3$	$x_{15}$	$x_{27}$	$x_{39}$	$x_{51}$	$x_{63}$	$x_{75}$	$x_{87}$	$x_{99}$	$x_{111}$	$x_{123}$	$x_{135}$
-------	----------	----------	----------	----------	----------	----------	----------	----------	-----------	-----------	-----------

9

$x_4$	$x_{16}$	$x_{28}$	$x_{40}$	$x_{52}$	$x_{64}$	$x_{76}$	$x_{88}$	$x_{100}$	$x_{112}$	$x_{124}$	$x_{136}$
-------	----------	----------	----------	----------	----------	----------	----------	-----------	-----------	-----------	-----------

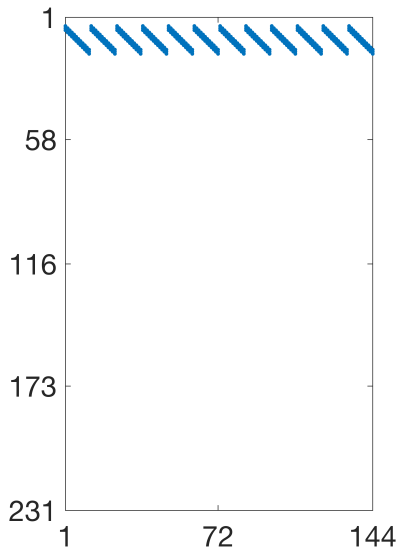


Matlab's `radon.m` routine produces the tomographic matrix using the pencil-beam model

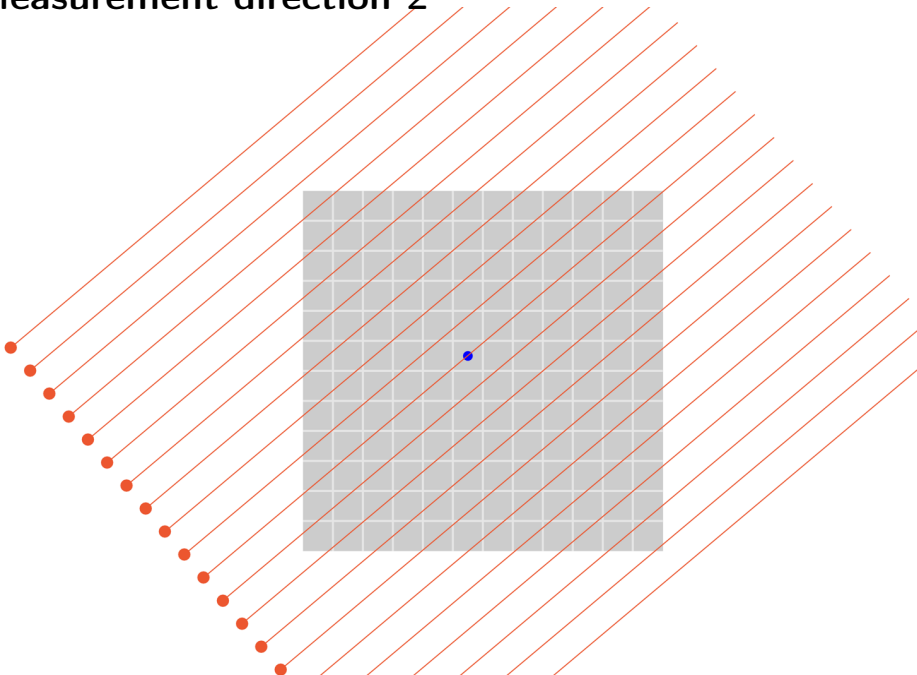
Here we see some columns starting from 13

	$x_{13}$	$x_{14}$	$x_{15}$	$x_{16}$	$x_{17}$	$x_{18}$	
Ray 1	...	0	0	0	0	0	...
Ray 2	...	0	0	0	0	0	...
Ray 3	...	0	0	0	0	0	...
Ray 4	...	0	0	0	0	0	...
Ray 5	...	0.125	0	0	0	0	...
Ray 6	...	0.750	0.125	0	0	0	...
Ray 7	...	0.125	0.750	0.125	0	0	...
Ray 8	...	0	0.125	0.750	0.125	0	...
Ray 9	...	0	0	0.125	0.750	0.125	0
Ray 10	...	0	0	0	0.125	0.750	0.125
	:	:	:	:	:	:	..

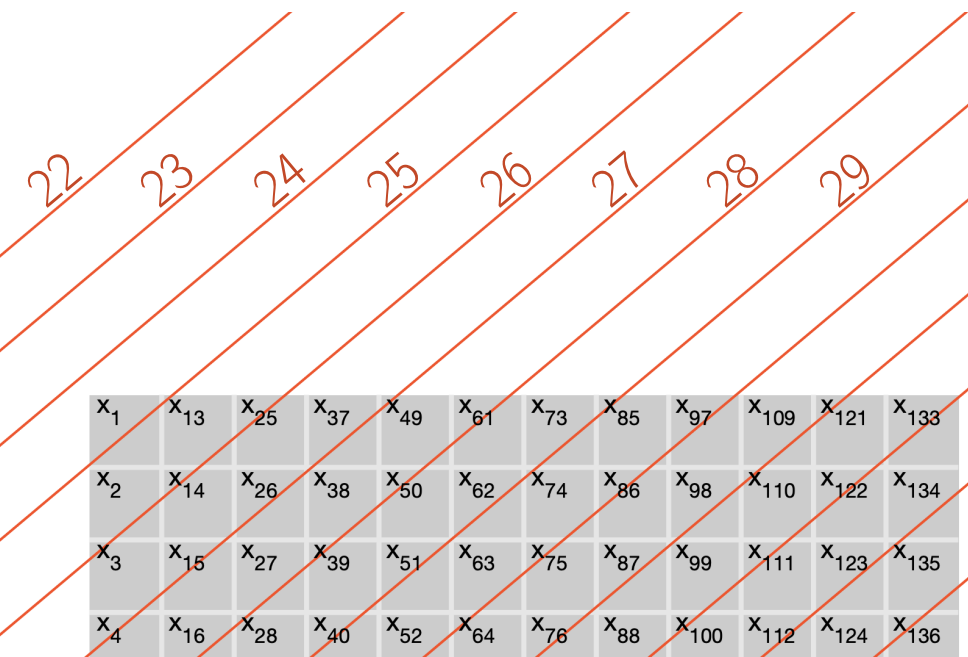
## Nonzero entries of matrix $A$ corresponding to the first measurement direction



## Measurement direction 2



# Paths of X-rays used in the second angle

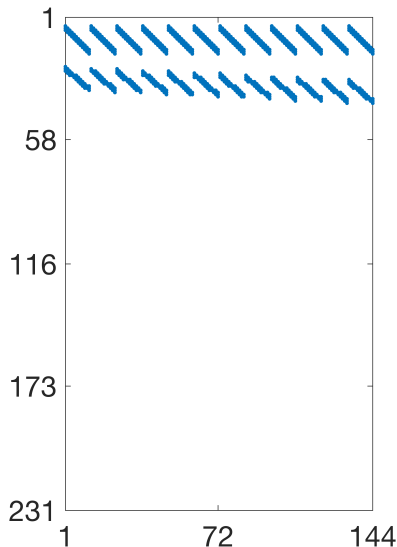


Matlab's `radon.m` routine produces the tomographic matrix using the pencil-beam model

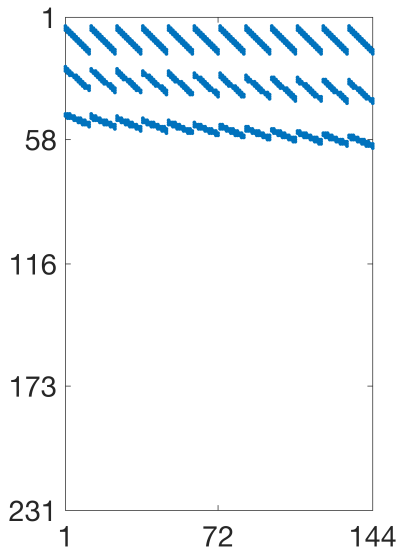
Matlab's `radon.m` routine produces the tomographic matrix using the pencil-beam model

	$x_{13}$	$x_{14}$	$x_{15}$	$x_{16}$	$x_{17}$	$x_{18}$
Ray 22	...	0	0	0	0	0
Ray 23	...	0	0	0	0	0
Ray 24	...	0	0	0	0	0
Ray 25	...	0.369	0	0	0	0
Ray 26	...	0.631	0.528	0.008	0	0
Ray 27	...	0	0.472	0.670	0.048	0
Ray 28	...	0	0	0.322	0.750	0.107
Ray 29	...	0	0	0	0.203	0.790
Ray 30	...	0	0	0	0.103	0.746
Ray 31	...	0	0	0	0	0.046
	...	...	...	...	...	...

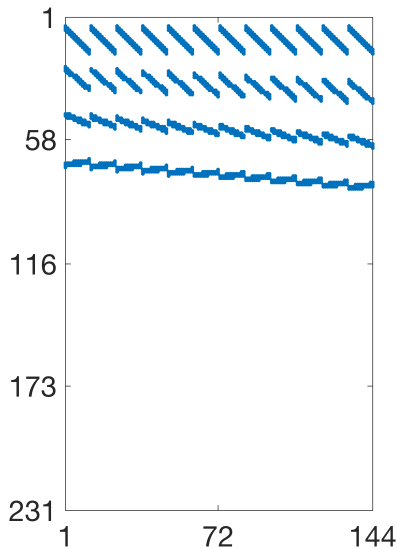
## Nonzero entries of matrix $A$ corresponding to the first two measurement directions



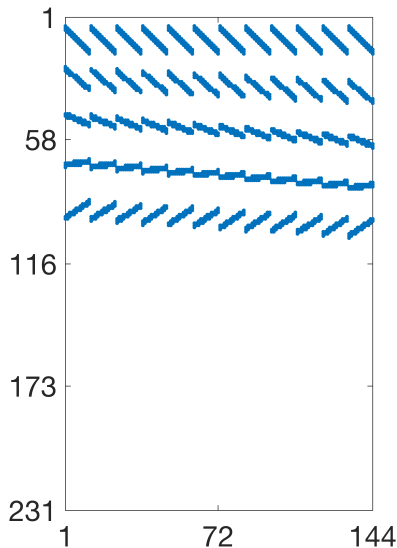
## Nonzero entries of matrix $A$ corresponding to measurement directions 1–3



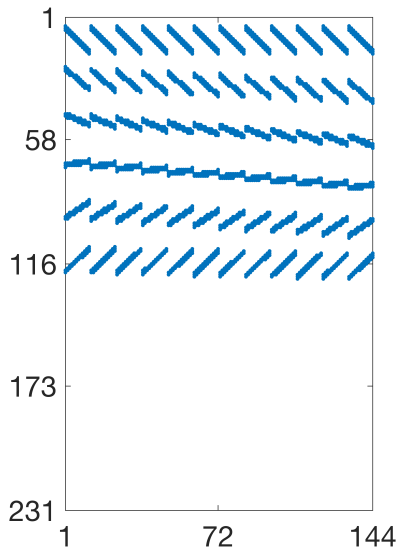
## Nonzero entries of matrix $A$ corresponding to measurement directions 1–4



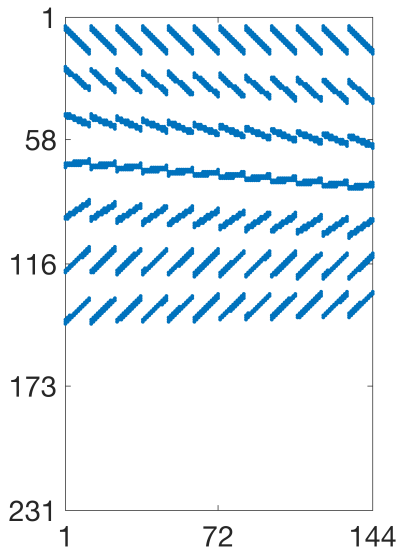
## Nonzero entries of matrix $A$ corresponding to measurement directions 1–5



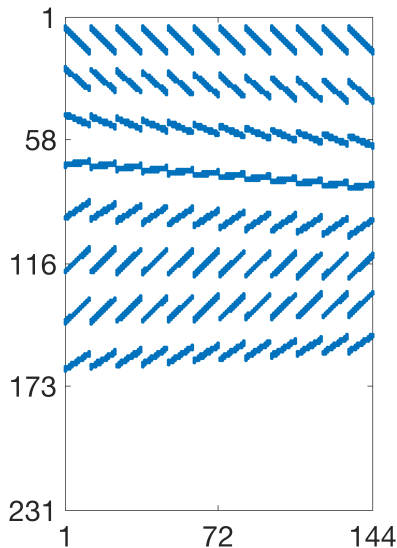
## Nonzero entries of matrix $A$ corresponding to measurement directions 1–6



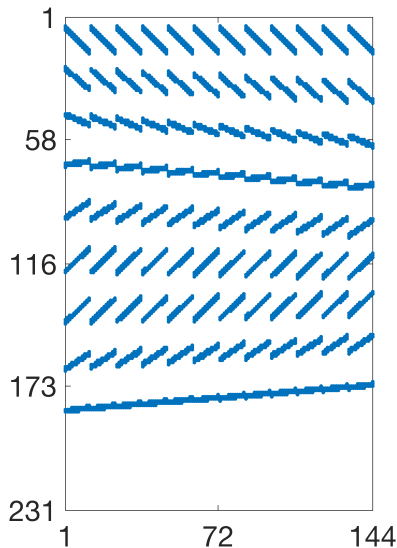
## Nonzero entries of matrix $A$ corresponding to measurement directions 1–7



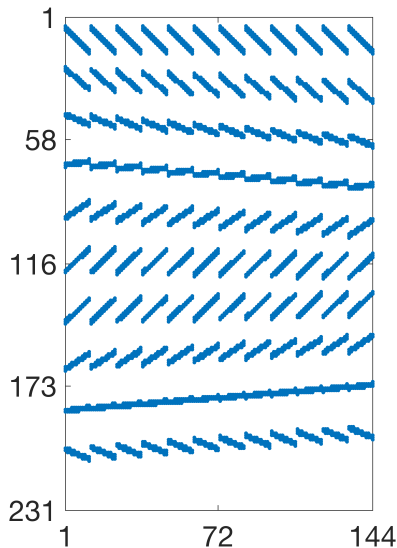
## Nonzero entries of matrix $A$ corresponding to measurement directions 1–8



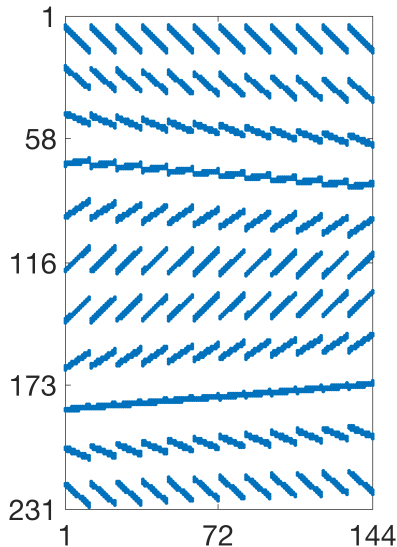
## Nonzero entries of matrix $A$ corresponding to measurement directions 1–9



## Nonzero entries of matrix $A$ corresponding to measurement directions 1–10



## Nonzero entries of matrix $A$ corresponding to measurement directions 1–11



# Outline

## Why pixel-based tomographic modelling?

Restricted time → sparse tomography

Restricted radiation dose → sparse tomography

Restricted money → sparse tomography

## The Beer-Lambert Law

## Pixel-based measurement model

Matrix model for sparse tomography

**Transpose of  $A$ : backprojection**

Ill-posedness of sparse tomography

Total variation regularization

## Regularization

Tikhonov regularization

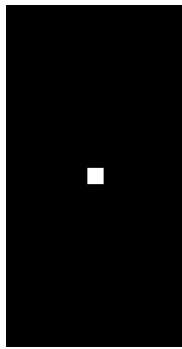
Total variation regularization

Frame-sparsity methods

Let's apply the transpose matrix  $A^T$  to a sinogram having just one nonzero entry

Sinogram in image form:

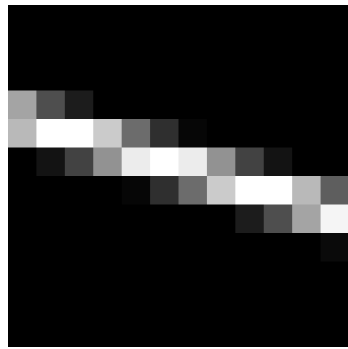
$$g \in \mathbb{R}^{21 \times 11}$$



Back-projection image:

$$A^T g \in \mathbb{R}^{12 \times 12}$$

$$\xrightarrow{A^T}$$

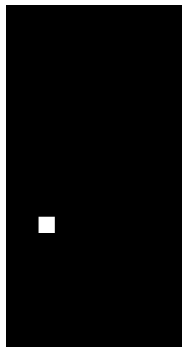


Note: you see the path of the X-ray indicated by the sinogram's white pixel.

Let's apply the transpose matrix  $A^T$  to a sinogram having just one nonzero entry

Sinogram in image form:

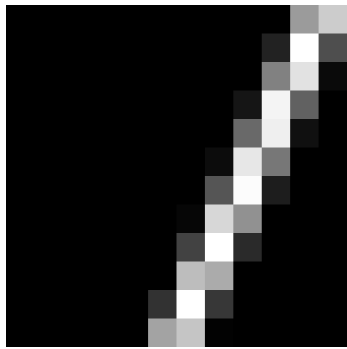
$$g \in \mathbb{R}^{21 \times 11}$$



Back-projection image:

$$A^T g \in \mathbb{R}^{12 \times 12}$$

$$\xrightarrow{A^T}$$

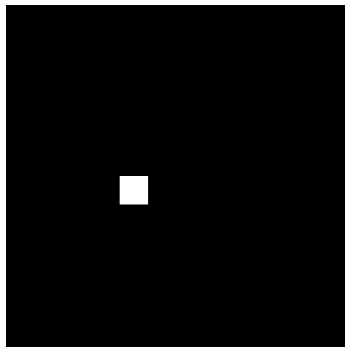


Note: you see the path of the X-ray indicated by the sinogram's white pixel.

**Consider a target with just one white pixel.  
The sinogram is like a sine curve!**

Target image:

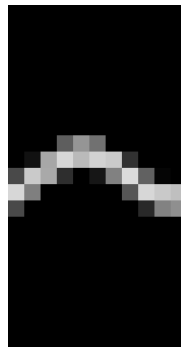
$$f \in \mathbb{R}^{12 \times 12}$$



$$\xrightarrow{A}$$

Sinogram in image form:

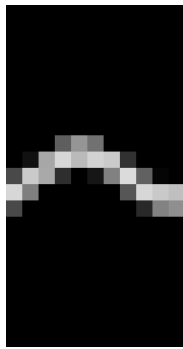
$$Af \in \mathbb{R}^{21 \times 11}$$



Let's apply the transpose matrix  $A^T$  to a sinogram arising from a target with just one white pixel

Sinogram in image form:

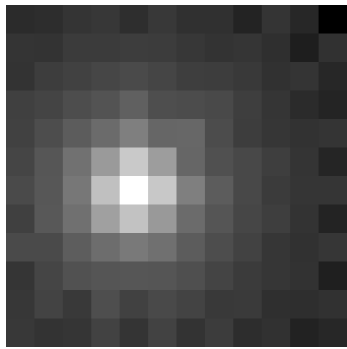
$$g \in \mathbb{R}^{21 \times 11}$$



Back-projection image:

$$A^T g \in \mathbb{R}^{12 \times 12}$$

$$\xrightarrow{A^T}$$



# Outline

## Why pixel-based tomographic modelling?

Restricted time → sparse tomography

Restricted radiation dose → sparse tomography

Restricted money → sparse tomography

## The Beer-Lambert Law

## Pixel-based measurement model

Matrix model for sparse tomography

Transpose of  $A$ : backprojection

## Ill-posedness of sparse tomography

Total variation regularization

## Regularization

Tikhonov regularization

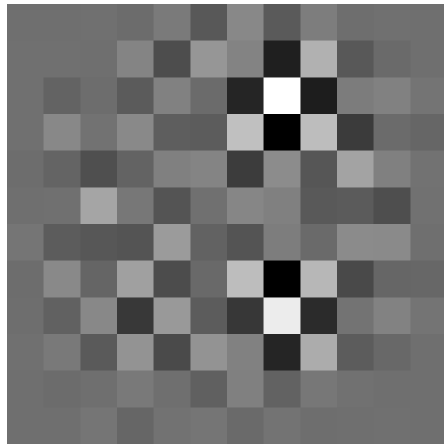
Total variation regularization

Frame-sparsity methods

# Naive reconstruction using the minimum norm solution from the normal equation $(A^T A)f^\dagger = A^T m$



Ground truth:  $12 \times 12$  resolution,  
values between 0 and 1

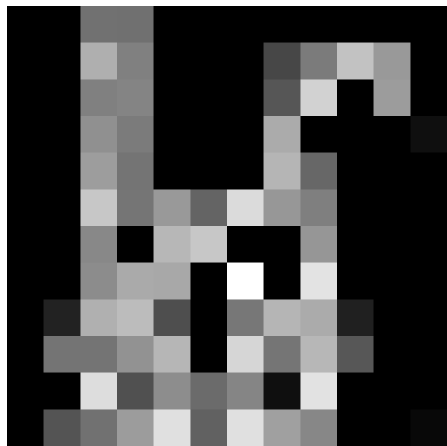


Reconstruction: minimum pixel value  
-294, maximum pixel value 380

# Naive reconstruction using the minimum norm solution with non-negativity constraint

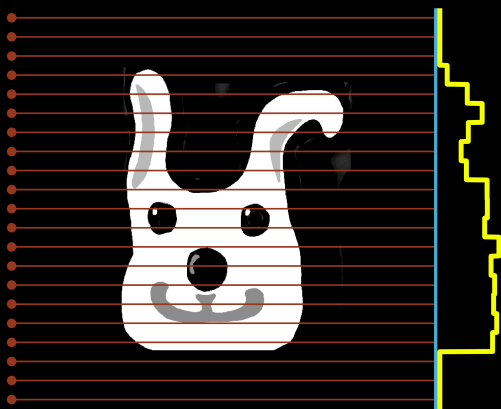


Ground truth:  $12 \times 12$  resolution,  
values between 0 and 1

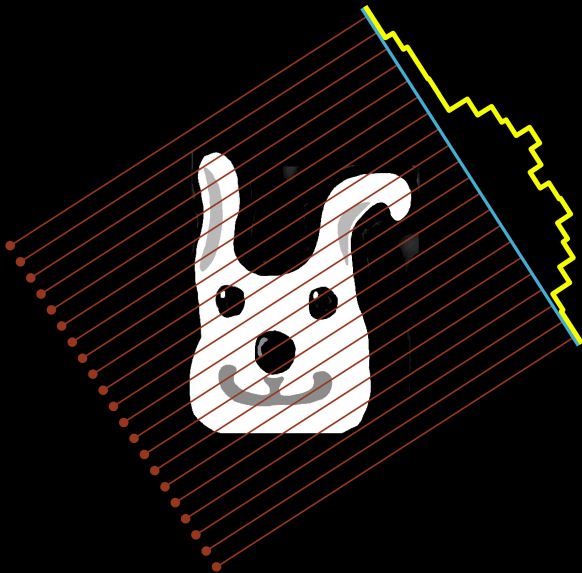


Reconstruction: minimum pixel value  
0, maximum pixel value 2.3

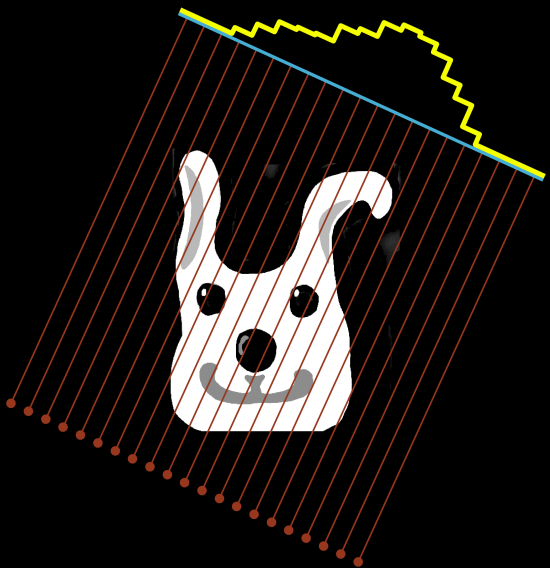
# Sinogram

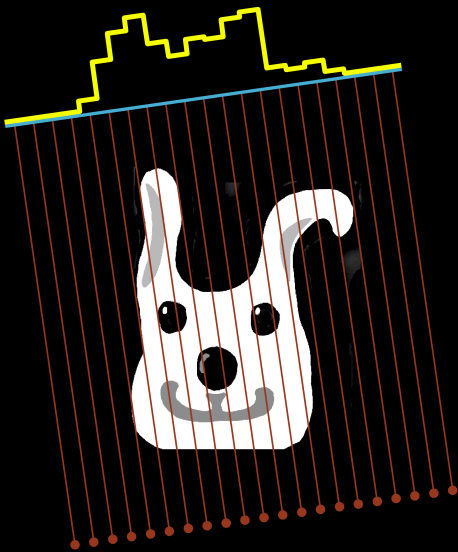


# Sinogram



# Sinogram

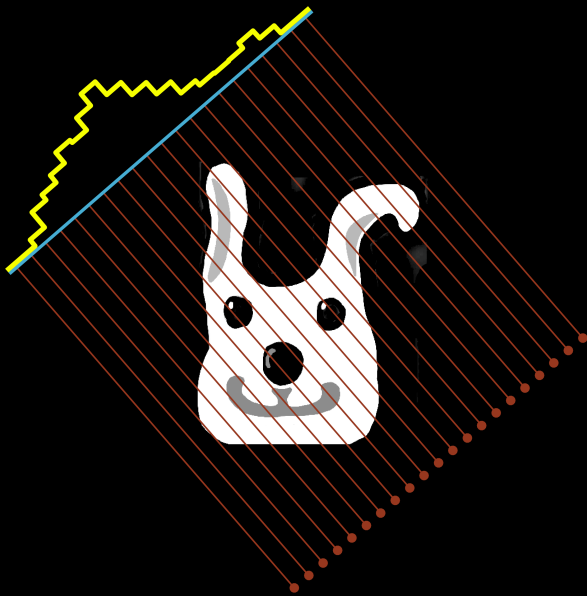




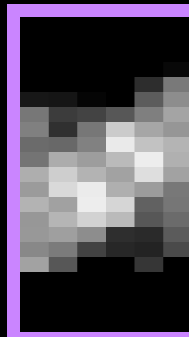
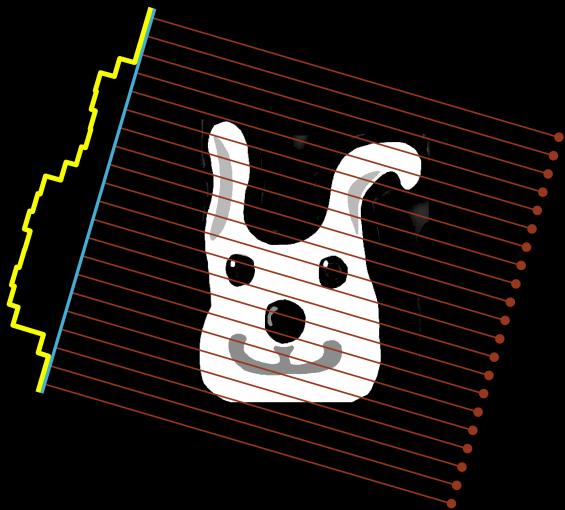
Sinogram



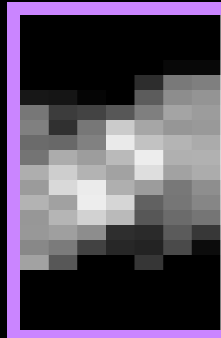
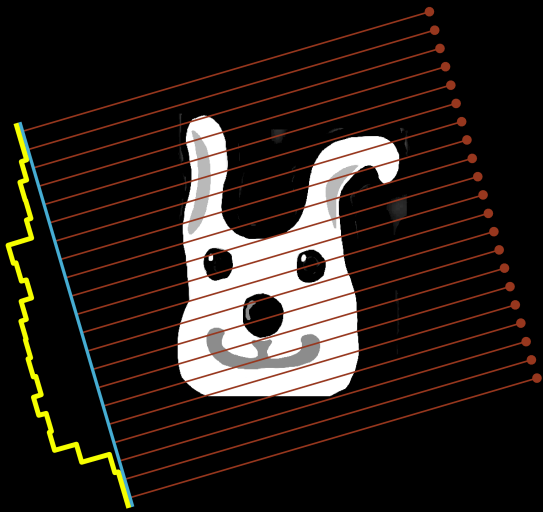
# Sinogram



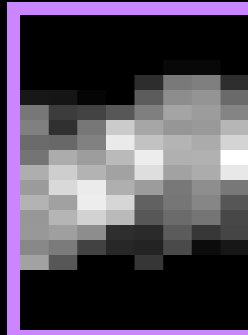
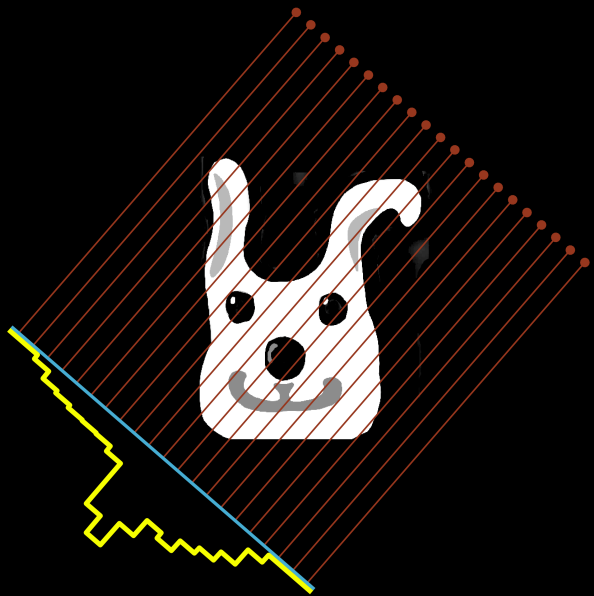
# Sinogram



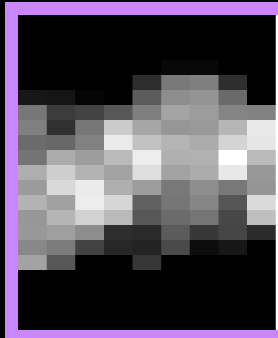
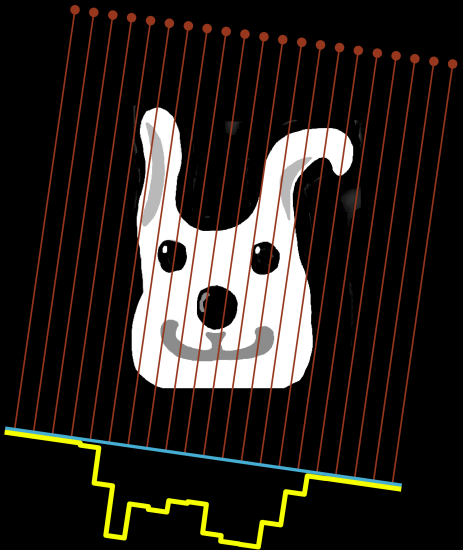
# Sinogram



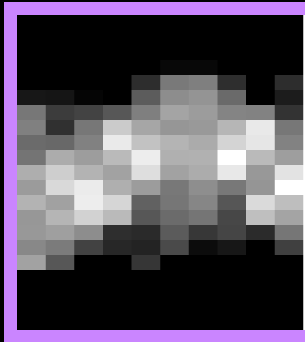
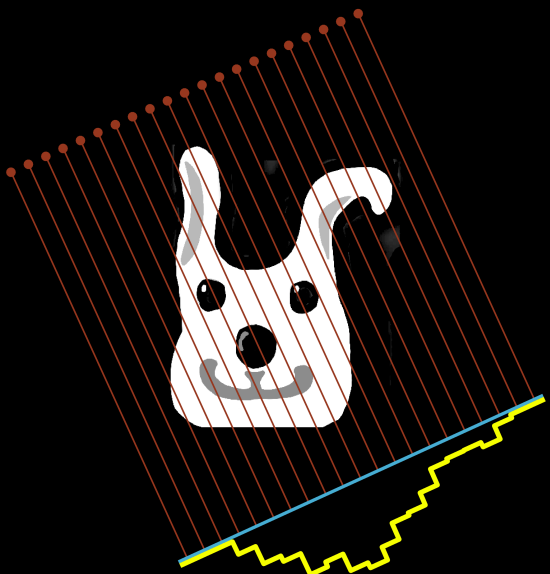
# Sinogram



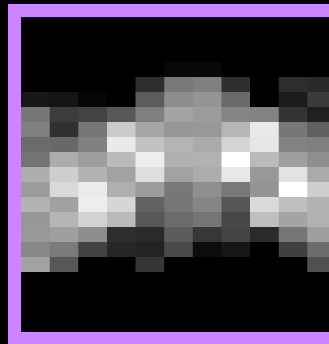
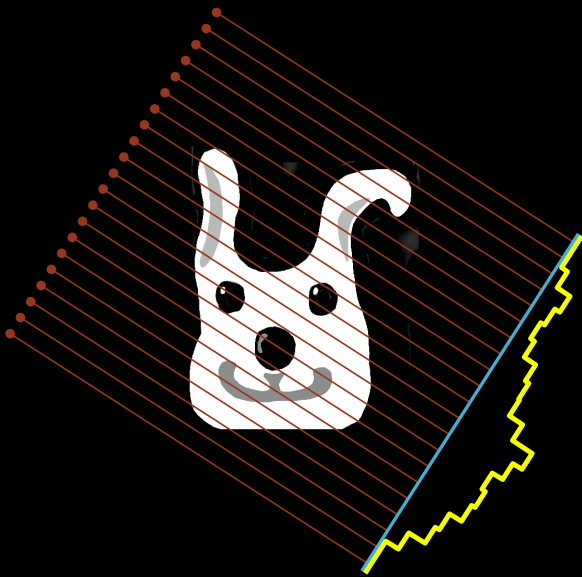
# Sinogram



# Sinogram



# Sinogram

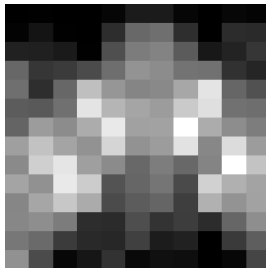


## III-posedness: first example of an almost-ghost

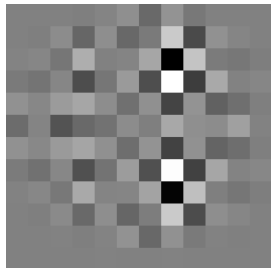


RRSE=134%

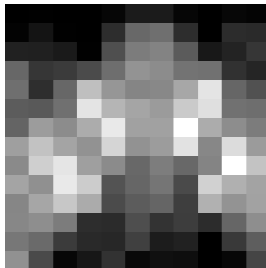
$$A \rightarrow$$



RRSE=0.1%



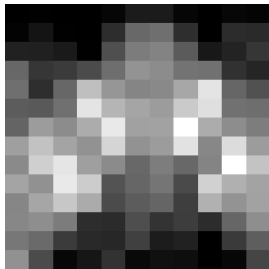
$$A \rightarrow$$



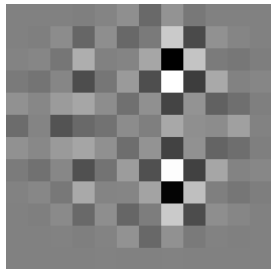
## III-posedness: first example of an almost-ghost



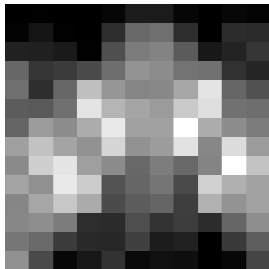
$$A \rightarrow$$



RRSE=134%



$$A \rightarrow$$



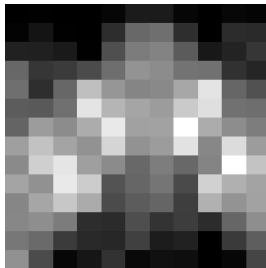
RRSE=0.1%

## III-posedness: second example of an almost-ghost

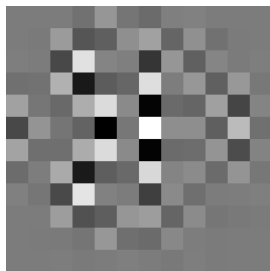


RRSE=134%

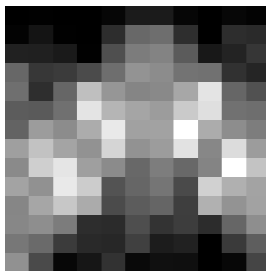
$$A \rightarrow$$



RRSE=0.1%



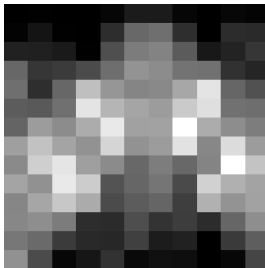
$$A \rightarrow$$



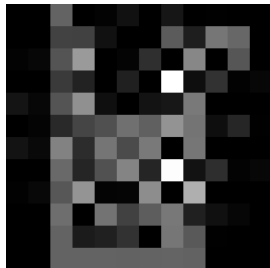
## Almost-ghost A with non-negativity constraint



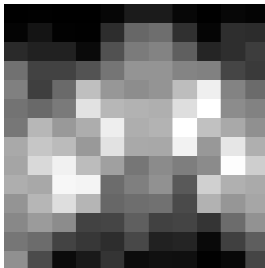
$$\xrightarrow{A}$$



RRSE=58%, SSIM=0.74



$$\xrightarrow{A}$$



RRSE=12%

**Singular Value Decomposition for  $k \times n$  matrix  $A$ :**  
 $A = UDV^T$  with  $UU^T = I = U^TU$  and  $VV^T = I = V^TV$

$$A = UDV^T = U \begin{bmatrix} d_1 & 0 & \cdots & 0 & & \cdots & 0 \\ 0 & d_2 & & & & & \vdots \\ \vdots & & \ddots & & & & \\ & & & d_r & & & \\ & & & & 0 & & \\ \vdots & & & & & \ddots & \vdots \\ 0 & \cdots & & & & \cdots & 0 \end{bmatrix} V^T$$

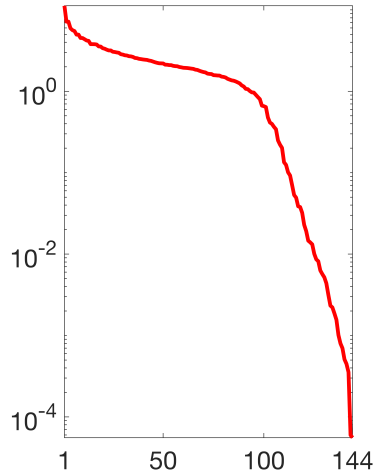
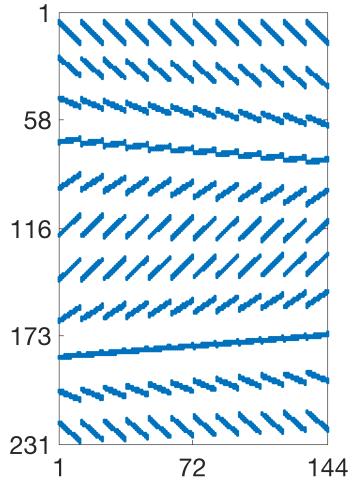
The singular values  $d_j$  satisfy  $d_1 \geq d_2 \geq \cdots \geq d_r > 0$   
and  $d_{r+1} = d_{r+2} = \cdots = d_{\min\{k,n\}} = 0$ . Note that  $r = \text{rank}(A)$ .

If  $n = k$  and all singular values are positive, then  $A$  is invertible.  
However, the *condition number*  $\text{cond}(A) := d_1/d_r$  may be large.  
In that case  $A^{-1}$  is a numerically unstable matrix.

**Singular value decomposition is  $A = UDV^T$ ,  
where  $U^T U = I = UU^T$  and  $V^T V = I = VV^T$**

$$A = \begin{array}{c} U \\ \hline 231 \times 231 \end{array} \quad \begin{array}{c} D \\ \hline 231 \times 144 \end{array} \quad \begin{array}{c} V^T \\ \hline 144 \times 144 \end{array}$$

In ill-posed problems, **singular values** decrease gradually from large to extremely small



# Outline

## Why pixel-based tomographic modelling?

Restricted time → sparse tomography

Restricted radiation dose → sparse tomography

Restricted money → sparse tomography

## The Beer-Lambert Law

## Pixel-based measurement model

Matrix model for sparse tomography

Transpose of  $A$ : backprojection

Ill-posedness of sparse tomography

Total variation regularization

## Regularization

Tikhonov regularization

Total variation regularization

Frame-sparsity methods

# Total variation (TV) regularization is a technique for preserving edges in the reconstruction

We consider calculating the minimizer of the TV functional

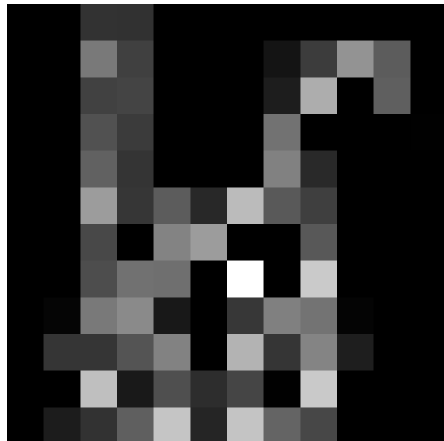
$$\begin{aligned} & \|Ax - m\|_2^2 + \alpha \{\|L_H x\|_1 + \|L_V x\|_1\} \\ = & \|Ax - m\|_2^2 + \alpha \left\{ \sum_j \sum_i \left( |x_{i(j+1)} - x_{ij}| + |x_{(i+1)j} - x_{ij}| \right) \right\} \end{aligned}$$

where  $L_H$  and  $L_V$  are horizontal and vertical first-order difference matrices. [Rudin, Osher and Fatemi 1992]

# Non-negative Total Variation (TV) regularization with too small parameter $\alpha = 0.0001$



Ground truth:  $12 \times 12$  resolution,  
values between 0 and 1

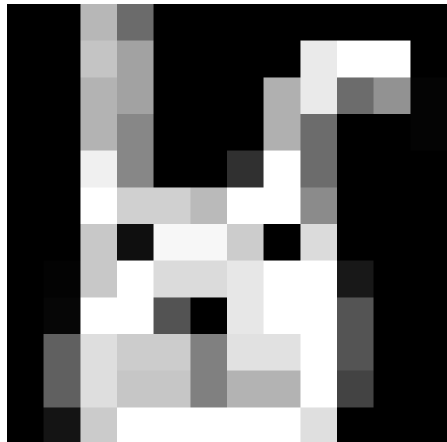


TV regularized reconstruction  
**RRSE=66% ,SSIM=0.40**

# Non-negative Total Variation (TV) regularization with pretty good parameter $\alpha = 0.3$



Ground truth:  $12 \times 12$  resolution,  
values between 0 and 1

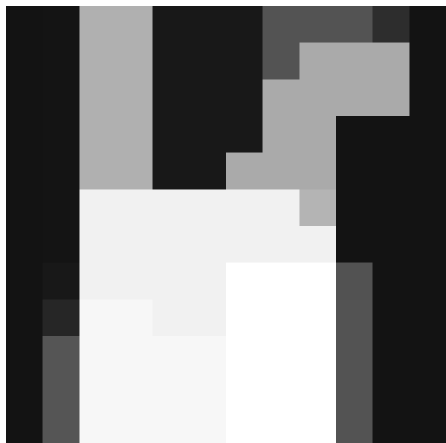


TV regularized reconstruction  
**RRSE=32% ,SSIM=0.87**

# Non-negative Total Variation (TV) regularization with too large parameter $\alpha = 4$



Ground truth:  $12 \times 12$  resolution,  
values between 0 and 1

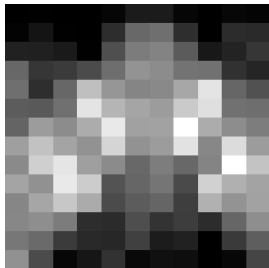


TV regularized reconstruction  
**RRSE=45% ,SSIM=0.70**

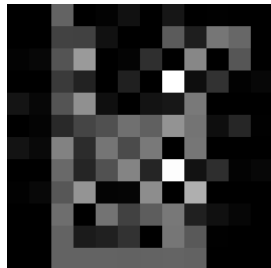
## Remember the nonnegative almost-ghost A



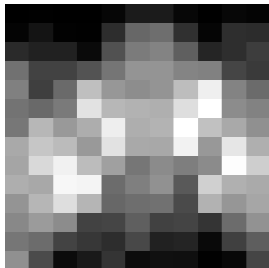
$$\xrightarrow{A}$$



RRSE=58%, SSIM=0.74



$$\xrightarrow{A}$$



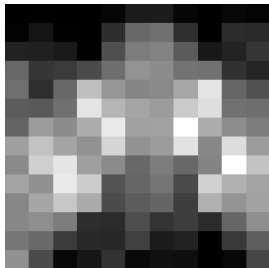
RRSE=12%

## TV reconstruction with $\alpha = 0.2$ , ghost A



RRSE=18%

$\xleftarrow{TV}$

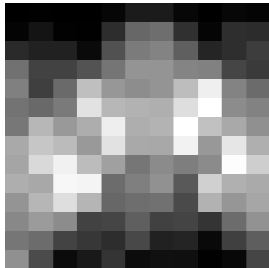


RRSE=12%



SSIM=0.85

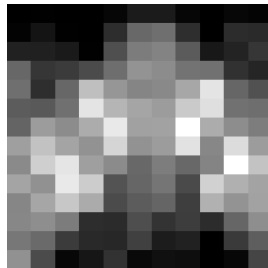
$\xleftarrow{TV}$



## Remember the nonnegative almost-ghost B

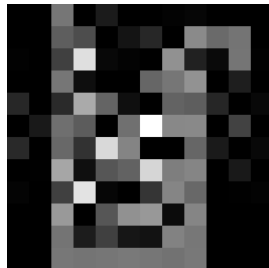


$$A \rightarrow$$

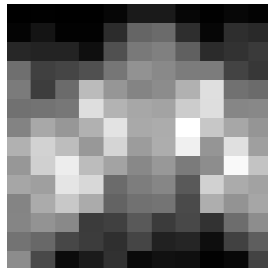


RRSE=58%, SSIM=0.74

RRSE=12%



$$A \rightarrow$$



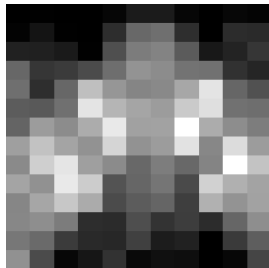
## TV reconstruction with $\alpha = 0.2$ , ghost B



$\xleftarrow{TV}$

SSIM=0.97

RRSE=19%

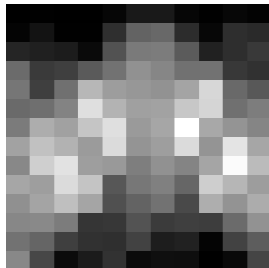


RRSE=12%



$\xleftarrow{TV}$

SSIM=0.91





A  
of  
Continuous  
Theory

## What can we expect to see from sparse data?

**THEOREM 4.2.** *A finite set of radiographs tells nothing at all.*

For some reason this theorem provokes merriment. It is so plainly one of those mathematical ideals untainted by any possibility of practical application.

[Cormack 1963], [Smith, Solmon & Wagner 1977, Theorem 4.2]

## Measuring the closeness of two images: root relative squared error (RRSE)

We need a number describing the similarity of images  $A$  and  $B$ . For example, we might want to compare a reconstruction to the ground truth, or quantify measurement noise amplitude as the difference between an ideal sinogram and a noisy sinogram.

The most classical method is RRSE, defined by

$$\text{RRSE}(A, B) = \frac{\sqrt{\sum_i \sum_j (A_{ij} - B_{ij})^2}}{\sqrt{\sum_i \sum_j A_{ij}^2}},$$

where  $i$  is row index and  $j$  is column index.

Note that  $\text{RRSE}(A, A) = 0$  means perfect fit, and that there is no upper bound for  $\text{RRSE}(A, B)$ .

## Measuring the closeness of two images: structural similarity index (SSIM)

RRSE has the downside of ignoring image structure: scrambling pixels makes no difference in RRSE. In imaging applications we need methods that better match the human perception of image quality.

One such option is SSIM, defined by

$$\text{SSIM}(A, B) = \frac{(2\mu_A\mu_B + c_1)(2\sigma_{AB} + c_2)}{(\mu_A^2\mu_B^2 + c_1)(\sigma_A^2 + \sigma_B^2 + c_2)},$$

where  $\mu_A, \mu_B$  are averages,  $\sigma_A, \sigma_B$  variances, and  $\sigma_{AB}$  the covariance of  $A$  and  $B$ . For constants  $c_1, c_2$  and other further details see [Wang, Bovik, Sheikh and Simoncelli 2004].

Note that  $\text{SSIM}(A, A) = 1$  means perfect fit, and that always  $-1 \leq \text{SSIM}(A, B) \leq 1$ .

# Outline

## Why pixel-based tomographic modelling?

Restricted time → sparse tomography

Restricted radiation dose → sparse tomography

Restricted money → sparse tomography

## The Beer-Lambert Law

## Pixel-based measurement model

Matrix model for sparse tomography

Transpose of  $A$ : backprojection

Ill-posedness of sparse tomography

Total variation regularization

## Regularization

Tikhonov regularization

Total variation regularization

Frame-sparsity methods

We saw before that for ill-posed inverse problems such as tomography, naive inversion fails

We need reconstruction methods that are robust against noise and modelling errors.

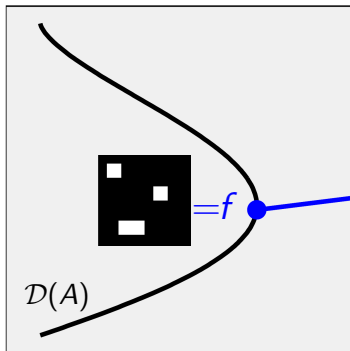
There are several methodologies for that, including

- ▶ variational regularization,
- ▶ Bayesian inversion,
- ▶ machine learning.

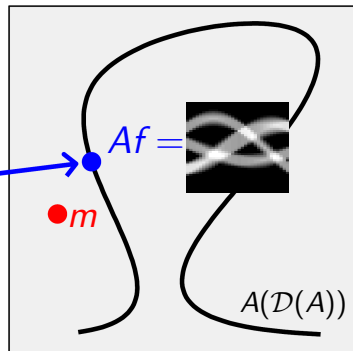
In these slides we will take a look at the first.

# Inverse problem of X-ray tomography: given noisy sinogram, find a stable approximation to $f$

Model space  $X = \mathbb{R}^{32 \times 32}$

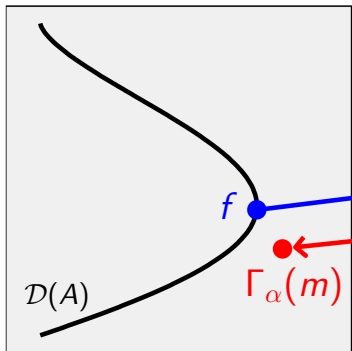


Data space  $Y = \mathbb{R}^{32 \times 49}$

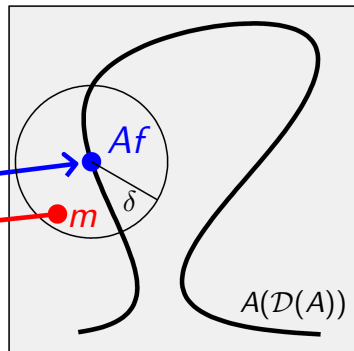


# Robust solution of ill-posed inverse problems requires regularization

Model space  $X = \mathbb{R}^{32 \times 32}$



Data space  $Y = \mathbb{R}^{39 \times 49}$



We need to define a family of continuous functions  $\Gamma_\alpha : Y \rightarrow X$  so that the reconstruction error  $\|\Gamma_{\alpha(\delta)}(m) - f\|_X$  vanishes asymptotically at the zero-noise level  $\delta \rightarrow 0$ .

You can find all the slides and codes of this course in GitHub

<https://github.com/ssiltane/BolognaWinterSchool2023>



# Outline

## Why pixel-based tomographic modelling?

Restricted time → sparse tomography

Restricted radiation dose → sparse tomography

Restricted money → sparse tomography

## The Beer-Lambert Law

## Pixel-based measurement model

Matrix model for sparse tomography

Transpose of  $A$ : backprojection

Ill-posedness of sparse tomography

Total variation regularization

## Regularization

Tikhonov regularization

Total variation regularization

Frame-sparsity methods

# Tikhonov regularization is the classical method for noise-robust tomographic reconstruction

Write a penalty functional

$$\Phi(f) = \|Af - m\|_2^2 + \alpha\|f\|_2^2,$$

where  $0 < \alpha < \infty$  is a regularization parameter. Define  $\Gamma_\alpha(m)$  by

$$\Phi(\Gamma_\alpha(m)) = \min_{f \in X} \{\Phi(f)\}.$$

We denote

$$\Gamma_\alpha(m) = \arg \min_{f \in X} \{\|Af - m\|_2^2 + \alpha\|f\|_2^2\}.$$

Tikhonov regularization can be expressed as filtering the singular values of the matrix  $A$

$$\Gamma_\alpha(\mathbf{m}) = V \begin{bmatrix} \frac{d_1}{d_1^2 + \alpha} & 0 & \dots & 0 \\ 0 & \ddots & & \vdots \\ \vdots & & \ddots & 0 \\ 0 & \dots & 0 & \frac{d_{\min\{k,n\}}}{d_{\min\{k,n\}}^2 + \alpha} \end{bmatrix} U^T \mathbf{m}$$

In large-scale computations it is better to use the formula

$$\Gamma_\alpha(\mathbf{m}) = (A^T A + \alpha I)^{-1} A^T \mathbf{m}$$

and an iterative solver such as the conjugate gradient method.

## Implementation of the matrix $A$ and its transpose $A^T$ (back-projection) are crucial things

In my small-scale two-dimensional Matlab examples I just use a brute-force trick for constructing  $A$  by calling the `radon.m` routine of Matlab repeatedly.

In practice it is important not to construct  $A$  or the back-projection operator  $A^T$  at all as matrices. Rather, one can use GPU-powered algorithms for calculating the maps  $f \mapsto Af$  and  $g \mapsto A^Tg$  for vectors  $f$  and  $g$  given by the solution method at each iteration.

For efficient matrix-free implementations, check out  
<https://tomopedia.github.io/>

# Outline

## Why pixel-based tomographic modelling?

Restricted time → sparse tomography

Restricted radiation dose → sparse tomography

Restricted money → sparse tomography

## The Beer-Lambert Law

## Pixel-based measurement model

Matrix model for sparse tomography

Transpose of  $A$ : backprojection

Ill-posedness of sparse tomography

Total variation regularization

## Regularization

Tikhonov regularization

Total variation regularization

Frame-sparsity methods

## Recall the $L^p$ norms for $\mathbb{R}^n$

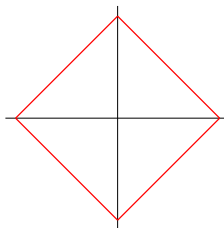
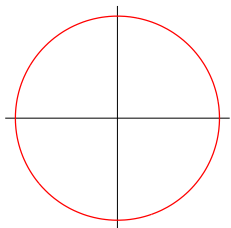
Let  $f \in \mathbb{R}^n$ . The  $L^p$  norms for  $1 \leq p < \infty$  are defined by

$$\|f\|_p = \left( \sum_{j=1}^n |f_j|^p \right)^{1/p}.$$

In particular we use the following two cases:

$$\|f\|_2^2 = \sum_{j=1}^n |f_j|^2,$$

$$\|f\|_1 = \sum_{j=1}^n |f_j|.$$



# Total variation (TV) regularization is a technique for preserving edges in the reconstruction

We consider calculating the minimizer of the TV functional

$$\begin{aligned} & \|Af - m\|_2^2 + \alpha \{\|L_H f\|_1 + \|L_V f\|_1\} \\ = & \|Af - m\|_2^2 + \alpha \left\{ \sum_j \sum_i \left( |f_{i(j+1)} - f_{ij}| + |f_{(i+1)j} - f_{ij}| \right) \right\} \end{aligned}$$

where  $L_H$  and  $L_V$  are horizontal and vertical first-order difference matrices. [Rudin, Osher and Fatemi 1992]

# Computational resources for total variation

You can find Matlab code for the above calculations at the following links. Many thanks to Professor **Kristian Bredies** for sharing his primal-dual codes!

[https://blog.fips.fi/tomography/x-ray/  
total-variation-regularization-for-x-ray-tomography/](https://blog.fips.fi/tomography/x-ray/total-variation-regularization-for-x-ray-tomography/)

Another computational method for the same problem is here:

[https://blog.fips.fi/tomography/x-ray/  
total-variation-regularization-for-x-ray-tomography-experimental-data/](https://blog.fips.fi/tomography/x-ray/total-variation-regularization-for-x-ray-tomography-experimental-data/)

The  $2 \times 2$  pixel example is here:

<https://github.com/ssiltane/SiltanenSparseTomography2x2>

Also, check out **Hendrik Dirks'** repository FlexBox:  
<https://github.com/HendrikMuenster/flexBox>

$$\text{TV tomography: } \arg \min_{f \in \mathbb{R}^n} \{ \|Af - m\|_2^2 + \alpha \|\nabla f\|_1 \}$$

- 1992 Rudin, Osher & Fatemi: denoise images by taking  $A = I$
- 1998 Delaney & Bresler
- 2001 Persson, Bone & Elmqvist
- 2003 Kolehmainen, S, Järvenpää, Kaipio, Koistinen, Lassas, Pirttilä & Somersalo (first TV work with measured X-ray data)
- 2006 Kolehmainen, Vanne, S, Järvenpää, Kaipio, Lassas & Kalke
- 2006 Sidky, Kao & Pan
- 2008 Liao & Sapiro
- 2008 Sidky & Pan
- 2008 Herman & Davidi
- 2009 Tang, Nett & Chen
- 2009 Duan, Zhang, Xing, Chen & Cheng
- 2010 Bian, Han, Sidky, Cao, Lu, Zhou & Pan
- 2011 Jensen, Jørgensen, Hansen & Jensen
- 2011 Tian, Jia, Yuan, Pan & Jiang
- 2012–present: hundreds of articles indicated by Google Scholar

# There are many computational approaches for computing the minimum

**Primal-dual algorithms** Bredies, Chambolle, Chan, Chen, Esser, Golub, Mulet, Nesterov, Zhang

**Thresholding** Candès, Chambolle, Chaux, Combettes, Daubechies, Defrise, DeMol, Donoho, Pesquet, Starck, Teschke, Vese, Wajs

**Bregman iteration** Cai, Burger, Darbon, Dong, Goldfarb, Mao, Osher, Shen, Xu, Yin, Zhang

**Splitting approaches** Chan, Esser, Fornasier, Goldstein, Langer, Osher, Schönlieb, Setzer, Wajs

**Nonlocal TV** Bertozzi, Bresson, Burger, Chan, Lou, Osher, Zhang

There is also the simple **quadratic programming** trick we used for the  $2 \times 2$  example before. That only works for relatively coarse pixelizations.

# Quadratic programming (QP) for TV regularization

The minimizer of the functional

$$\arg \min_{f \in \mathbb{R}_+^n} \left\{ \|Af - m\|_2^2 + \alpha \|L_H f\|_1 + \alpha \|L_V f\|_1 \right\}$$

can be transformed into the standard form

$$\arg \min_{z \in \mathbb{R}^{5n}} \left\{ \frac{1}{2} z^T Q z + c^T z \right\}, \quad z \geq 0, \quad E z = b,$$

where  $Q$  is symmetric and  $E$  implements equality constraints.

Large-scale primal-dual interior point QP method was developed in Kolehmainen, Lassas, Niinimäki & S (2012) and Hämäläinen, Kallonen, Kolehmainen, Lassas, Niinimäki & S (2013).

$$\text{Reduction to } \arg \min_{z \in \mathbb{R}^{5n}} \left\{ \frac{1}{2} z^T Q z + c^T z \right\}$$

Denote horizontal and vertical differences by

$$L_H f = u_H^+ - u_H^- \quad \text{and} \quad L_V f = u_V^+ - u_V^-,$$

where  $u_H^\pm, u_V^\pm \geq 0$ . TV minimization is now

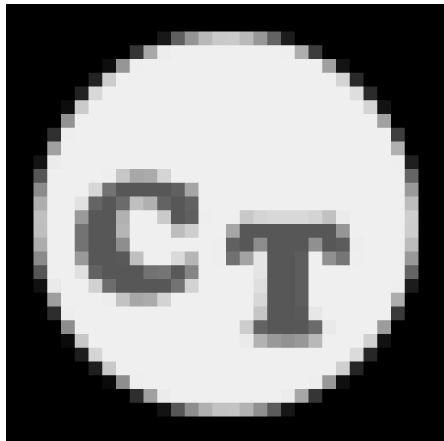
$$\arg \min_{f \in \mathbb{R}_+^n} \left\{ f^T A^T A f - 2f^T A^T m + \alpha \mathbf{1}^T (u_H^+ + u_H^- + u_V^+ + u_V^-) \right\},$$

where  $\mathbf{1} \in \mathbb{R}^n$  is vector of all ones. Further, we denote

$$z = \begin{bmatrix} f \\ u_H^+ \\ u_H^- \\ u_V^+ \\ u_V^- \end{bmatrix}, \quad Q = \begin{bmatrix} \frac{1}{\sigma^2} A^T A & 0 & 0 & 0 & 0 \\ 0 & 0 & 0 & 0 & 0 \\ 0 & 0 & 0 & 0 & 0 \\ 0 & 0 & 0 & 0 & 0 \\ 0 & 0 & 0 & 0 & 0 \end{bmatrix}, \quad c = \begin{bmatrix} -2A^T m \\ \alpha \mathbf{1} \\ \alpha \mathbf{1} \\ \alpha \mathbf{1} \\ \alpha \mathbf{1} \end{bmatrix}.$$

## Non-negative TV regularization

$$\arg \min_{f \in \mathbb{R}_+^n} \left\{ \|Af - m\|_2^2 + \alpha \|\nabla f\|_1 \right\}$$

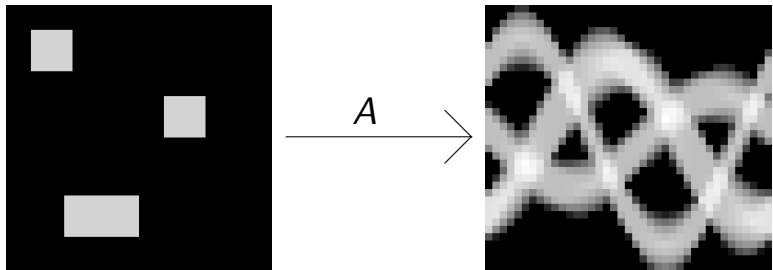


Original phantom sampled at  
32×32 resolution



TV regularized reconstruction  
Relative square norm error 7%

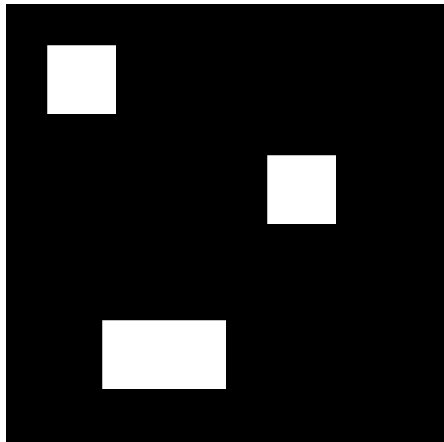
Let's consider a square phantom



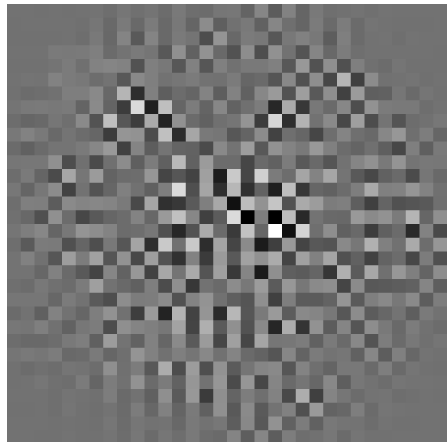
$$f \in \mathbb{R}^{32 \times 32}$$

$$Af \in \mathbb{R}^{49 \times 39}$$

## Naive reconstruction using the Moore-Penrose pseudoinverse; data has 0.1% relative noise



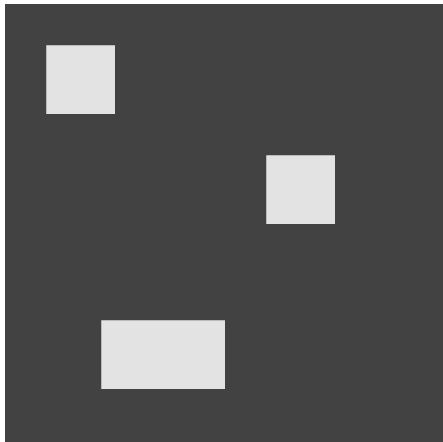
Original phantom, values between zero (black) and one (white)



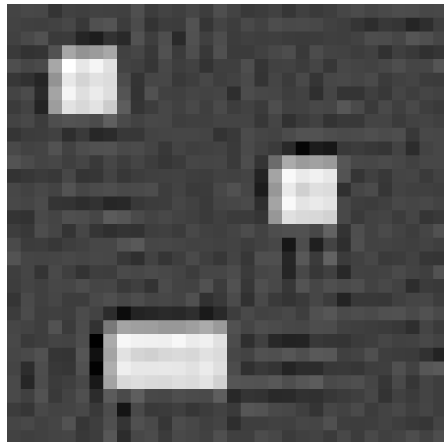
Naive reconstruction with minimum -14.9 and maximum 18.5

# Standard Tikhonov regularization

$$\arg \min_{f \in \mathbb{R}^n} \left\{ \|Af - m\|_2^2 + \alpha \|f\|_2^2 \right\}$$



Original phantom

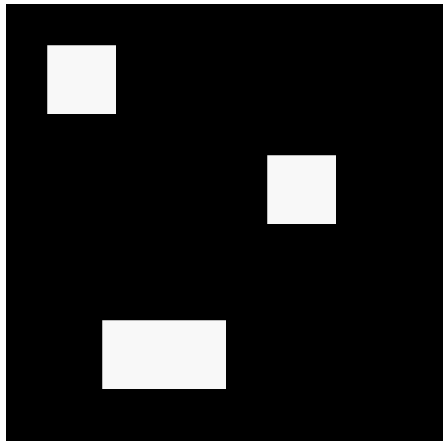


Reconstruction

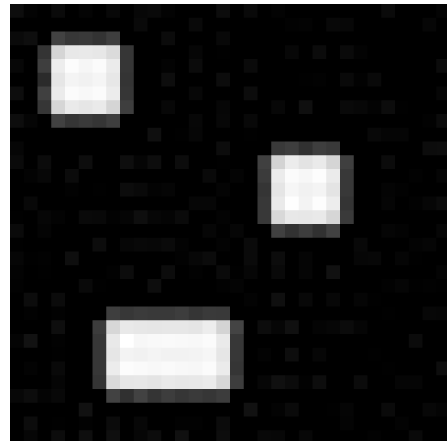
Relative square norm error 35%

# Constrained Tikhonov regularization

$$\arg \min_{f \in \mathbb{R}_+^n} \left\{ \|Af - m\|_2^2 + \alpha \|f\|_2^2 \right\}$$



Original phantom

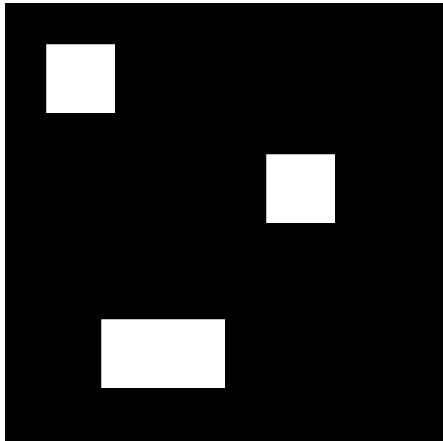


Reconstruction

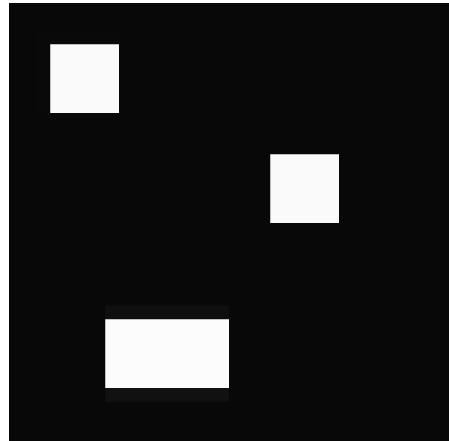
Relative square norm error 13%

## Constrained total variation (TV) regularization

$$\arg \min_{f \in \mathbb{R}_+^n} \left\{ \|Af - m\|_2^2 + \alpha \{\|L_h f\|_1 + \|L_v f\|_1\} \right\}$$



Original phantom



TV regularized reconstruction  
Relative square norm error 3%

In variational regularization, the penalty term expresses *a priori* knowledge about the unknown

Standard Tikhonov regularization:

$$\arg \min_{f \in \mathbb{R}^n} \left\{ \|Af - m\|_2^2 + \alpha \|f\|_2^2 \right\}$$

Non-negativity constrained Tikhonov regularization:

$$\arg \min_{f \in \mathbb{R}_+^n} \left\{ \|Af - m\|_2^2 + \alpha \|f\|_2^2 \right\}$$

Non-negativity constrained Total Variation (TV) regularization:

$$\arg \min_{f \in \mathbb{R}_+^n} \left\{ \|Af - m\|_2^2 + \alpha \|\nabla f\|_1 \right\}$$

# Outline

## Why pixel-based tomographic modelling?

Restricted time → sparse tomography

Restricted radiation dose → sparse tomography

Restricted money → sparse tomography

## The Beer-Lambert Law

## Pixel-based measurement model

Matrix model for sparse tomography

Transpose of  $A$ : backprojection

Ill-posedness of sparse tomography

Total variation regularization

## Regularization

Tikhonov regularization

Total variation regularization

Frame-sparsity methods

# Daubechies, Defrise and de Mol introduced a revolutionary inversion method in 2004

Consider the sparsity-promoting variational regularization

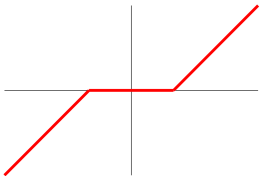
$$\arg \min_{f \in \mathbb{R}^n} \left\{ \|Af - m\|_2^2 + \mu \|Wf\|_1 \right\},$$

where  $W$  is an orthonormal wavelet transform. The minimizer can be computed using the iteration

$$f_{j+1} = W^{-1} S_\mu W \left( f_j + A^T(m - Af_j) \right),$$

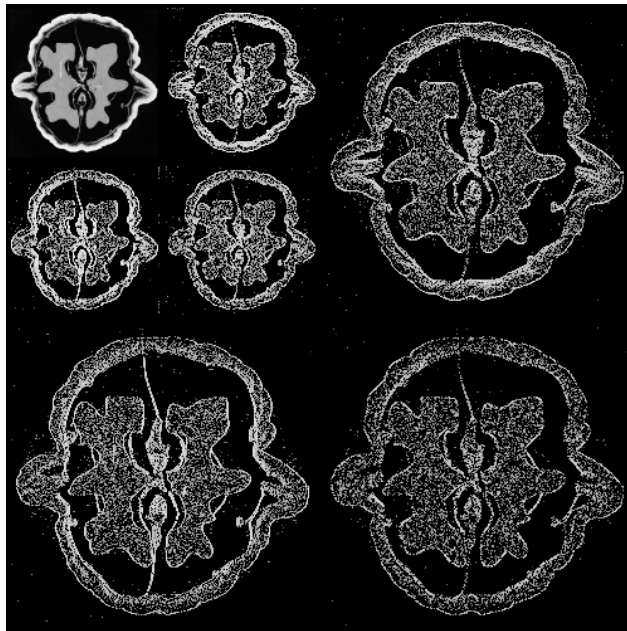
where the soft-thresholding operation

$$S_\mu(x) = \begin{cases} x + \frac{\mu}{2} & \text{if } x \leq -\frac{\mu}{2}, \\ 0 & \text{if } |x| < \frac{\mu}{2}, \\ x - \frac{\mu}{2} & \text{if } x \geq \frac{\mu}{2}, \end{cases}$$

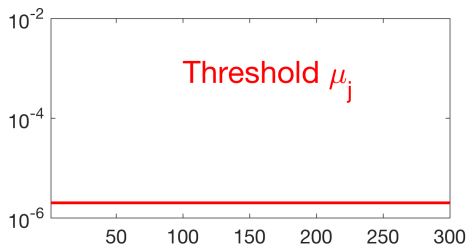
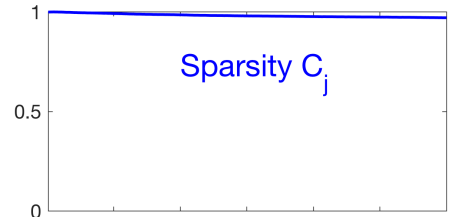
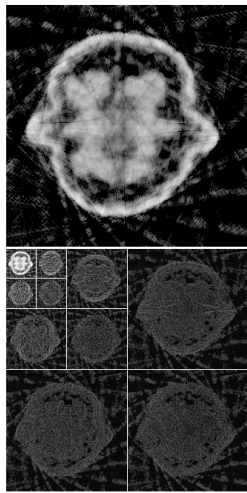


is applied to each wavelet coefficient separately.

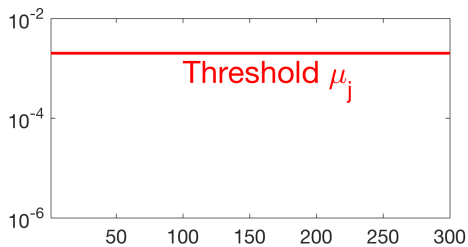
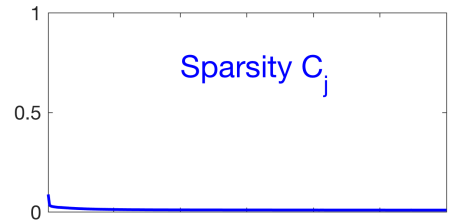
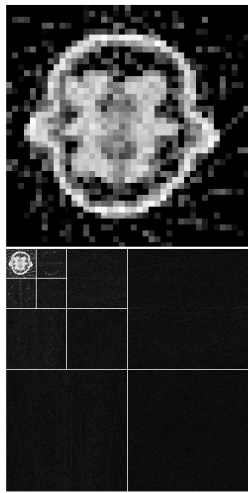
# Illustration of the Haar wavelet transform



# How to choose the thresholding parameter $\mu$ ? Here it is too small.



How to choose the thresholding parameter  $\mu$ ?  
Here it is too large.



# Automatic parameter choice using controlled wavelet-domain sparsity (CWDS)

Assume given the *a priori* sparsity level  $0 \leq \mathcal{C}_{\text{pr}} \leq 1$ .

Denote by  $\mathcal{C}_j$  the sparsity of the  $j$ th iterate  $f_j \in \mathbb{R}^n$ :

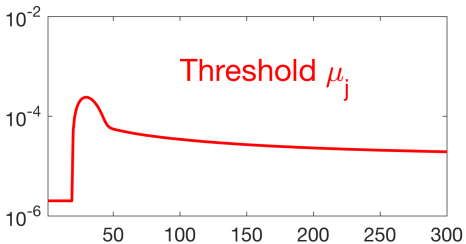
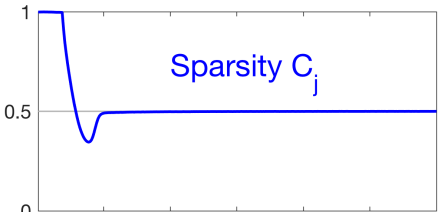
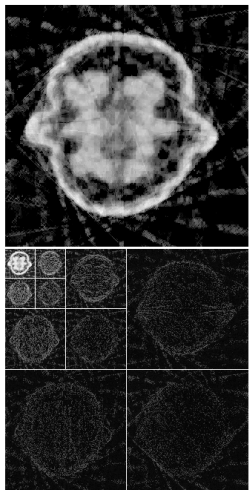
$$\mathcal{C}_j = (\text{number of nonzero elements in } Wf_j \in \mathbb{R}^n) / n.$$

The CWDS iteration is based on proportional-integral-derivative (PID) controllers:

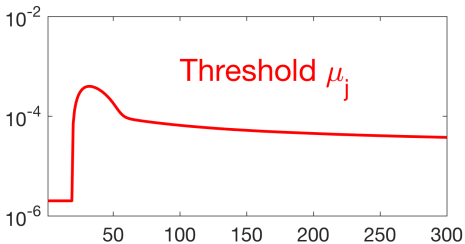
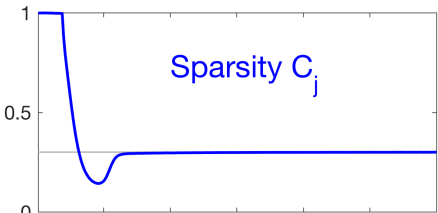
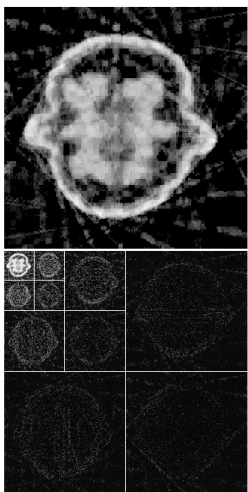
$$\mu^{(i+1)} = \mu^{(i)} + \beta(\mathcal{C}^{(i)} - \mathcal{C}_{\text{pr}}).$$

[Purisha, Rimpeläinen, Bubba & S 2018]

# CWDS choice of the thresholding parameter $\mu$



# CWDS choice of the thresholding parameter $\mu$



# We modify the method so that non-negativity constraint has rigorous mathematical foundation

The minimizer

$$\operatorname{argmin}_{\substack{\mathbf{f} \in \mathbb{R}_+^n}} \left\{ \frac{1}{2} \|\mathbf{A}\mathbf{f} - \mathbf{m}\|_2^2 + \mu \|\mathbf{W}\mathbf{f}\|_1 \right\}$$

can be computed using this iteration:

$$\mathbf{y}^{(i+1)} = \mathbb{P}_C \left( \mathbf{f}^{(i)} - \tau \nabla g(\mathbf{f}^{(i)}) - \lambda \mathbf{W}^T \mathbf{v}^{(i)} \right)$$

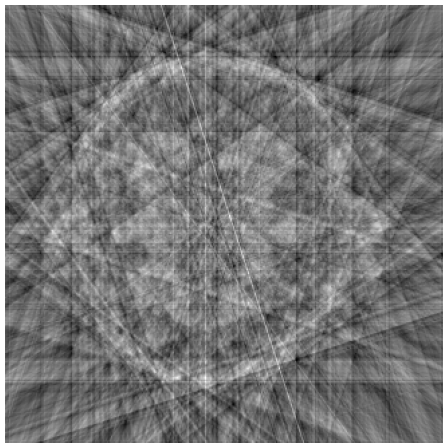
$$\mathbf{v}^{(i+1)} = (I - S_\mu) (\mathbf{W}\mathbf{y}^{(i+1)} + \mathbf{v}^{(i)})$$

$$\mathbf{f}^{(i+1)} = \mathbb{P}_C \left( \mathbf{f}^{(i)} - \tau \nabla g(\mathbf{f}^{(i)}) - \lambda \mathbf{W}^T \mathbf{v}^{(i+1)} \right)$$

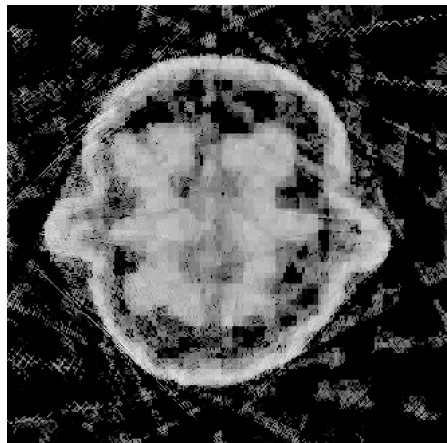
where  $\tau > 0$ ,  $\lambda > 0$  and  $g(\mathbf{f}) = \frac{1}{2} \|\mathbf{A}\mathbf{f} - \mathbf{m}\|_2^2$ . Here  $\mathbb{P}_C$  denotes projection to the non-negative “quadrant.”

[Loris & Verhoeven 2011], [Chen, Huang & Zhang 2016]

# Sparse-data reconstruction of the walnut using Haar wavelet sparsity



Filtered back-projection



Constrained Besov regularization

$$\arg \min_{f \in \mathbb{R}_+^n} \left\{ \|Af - m\|_2^2 + \alpha \|f\|_{B_{11}^1} \right\}$$

# Computational resources for frame sparsity

You can find Matlab code for the above calculations at

[https://blog.fips.fi/tomography/x-ray/  
automatic-regularization-parameter-selection-controlled-  
wavelet-domain-sparsity/](https://blog.fips.fi/tomography/x-ray/automatic-regularization-parameter-selection-controlled-wavelet-domain-sparsity/)



## A note on Besov function spaces

We are using the norm  $\|Wf\|_1$  as a regularizer. Here  $Wf$  is the set of wavelet coefficientd of  $f$ , organized as a vector. What kind of norm is that?

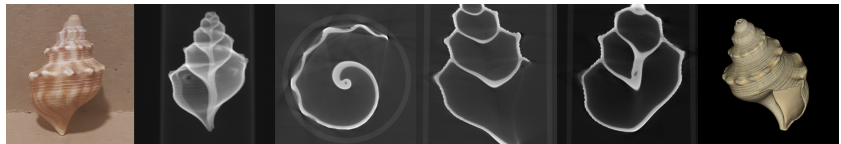
There is a theory of function spaces  $B_{pq}^s$ , named after Oleg Besov. They consist of functions having a specific order  $s$  of weak differentiability and certain integrability properties  $(p, q)$ . In particular, these two norms are equivalent:

$$\|Wf\|_1 \cong \|f\|_{B_{11}^1}.$$

This is nice since  $B_{11}^1$  is concerned with  $L^1$  norms of first derivatives, a bit like TV, but more manageable as a space than TV or BV.

For information about these functions, check out the book *Function Spaces and Wavelets on Domains (EMS 2008)* by Hans Triebel.

# X-ray tomographic datasets



Finnish Inverse Problems Society: <https://www.fips.fi/dataset.php>

Tomobank: <https://tomobank.readthedocs.io/en/latest/>

# SCIENCE



## CURIOSITY AT ALL SCALES